RM No. A9B16

NACA

RESEARCH MEMORANDUM

WIND-TUNNEL INVESTIGATION OF A TAILLESS TRIANGULAR-WING FIGHTER AIRCRAFT AT MACH NUMBERS FROM 0.5 TO 1.5

By Leslie F. Lawrence and James L. Summers

Ames Aeronautical Laboratory
Moffett Field, Calif.

NATIONAL ADVISORY COMMITTEE FOR AERONAUTICS

WASHINGTON
June 24, 1949

NACA RM No. A9B16

NATIONAL ADVISORY COMMITTEE FOR AERONAUTICS

RESEARCH MEMORANDUM

WIND-TUNNEL INVESTIGATION OF A TAILLESS TRIANGULAR-WING FIGHTER AIRCRAFT AT MACH NUMBERS FROM 0.5 TO 1.5

By Leslie F. Lawrence and James L. Summers

SUMMARY

A wind-tunnel investigation has been made to determine the respective variations with Mach number of the static longitudinal stability, the drag, and the effectiveness of a constant-chord control surface for a tailless fighter aircraft employing a triangular wing of aspect ratio 2.31. These characteristics were determined for the airplane provided with two alternative air entries: an external compression, or shock diffuser, entry and an open nose entry. Measurements of lift, drag, and pitching moment were made through an angle-of-attack range of -4° to $+14^{\circ}$, and over a range of Mach numbers from 0.5 to 1.52 (excluding the region from 0.95 to 1.20) with corresponding Reynolds numbers, based on the mean aerodynamic chord, ranging from 0.8×10^{6} to 1.0×10^{6}.

The models with either type of entry became increasingly stable with increasing Mach number. (The quarter point of the mean aerodynamic chord was the reference for pitching-moment coefficients.)

The variation with Mach number of the minimum drag coefficient of the model was characteristic of that for triangular wings of comparable aspect ratio, the minimum drag coefficient increasing approximately 100 percent between 0.85 and 1.20 Mach number. A substantial portion of the minimum drag coefficient was contributed by the fuselage of the model.

With increasing Mach number up to 0.95, the lift and pitching-moment effectiveness of the control surface remained substantially constant. The lift effectiveness at supersonic Mach numbers was approximately one-half the subsonic value. The pitching-moment effectiveness decreased continuously from the subsonic value to approximately 50 percent of this value at 1.52 Mach number.

INTRODUCTION

The triangular wing of low aspect ratio possesses characteristics which make it appear suitable for use on fighter aircraft designed to operate at moderate supersonic Mach numbers. Information, however, is currently lacking concerning the stability and control characteristics of a supersonic airplane with this type of wing. The present investigation was conducted to determine the variation with Mach number of the longitudinal stability, drag, and control-surface effectiveness of a model of a representative fighter aircraft employing a triangular wing with constant-chord trailing-edge control surfaces. The model was equipped with an external compression, or shock diffuser, air entry.

The investigation of the drag characteristics included determination of the increments of drag contributed by the principal components of the configuration. In addition, some measure of the effect of an open nose air entry on the longitudinal static stability and the drag of the model was determined.

SYMBOLS

a.c.	aerodynamic center
C_D	drag coefficient, based on the corrected balance drag reading which includes the drag due to internal flow
$C_{D_{min}}$	minimum drag coefficient
C_{D_I}	internal drag coefficient, based on the difference of the total momentum of the internal flow between the outlet of the body and the entering free-stream tube
C_L	lift coefficient
$\left(\frac{dC_L}{d\delta_e}\right)_{av}$	average values of rate of change of lift coefficient with control-surface deflection, per degree
$C_{m_{\bar{c}/4}}$	pitching-moment coefficient about quarter-chord point of the mean aerodynamic chord
$\left(\frac{dC_m}{d\delta_e}\right)_{av}$	average values of rate of change of pitching-moment coefficient with control-surface deflection, per degree

c	wing chord, feet
$\bar{c}$	mean aerodynamic chord of gross triangular wing area $\left(\frac{\int c^2\,dy}{\int c\,dy}\right)$, feet
M	Mach number
$\frac{m_1}{m_o}$	mass-flow coefficient
m_1	mass flow in duct, slugs per second
m_o	mass flow in free-stream tube with cross-sectional area equal to duct entrance area, slugs per second
q	free-stream dynamic pressure, pounds per square foot
R	Reynolds number, based on mean aerodynamic chord
y	spanwise distance, feet
α	angle of attack, degrees
δ_e	control-surface deflection, degrees

APPARATUS AND TESTS

The investigation was conducted in the Ames 1- by 3-1/2-foot high-speed wind tunnel, which is equipped with a flexible nozzle to permit a variation of Mach number from 0 to approximately 1.50. (See fig. 1.) A three-component strain-gage balance was employed to measure lift, drag, and pitching moment.

Three-view drawings and photographs of the models tested are shown in figures 2 and 3. These models were reproductions of probable configurations of a fighter designed to operate at high subsonic and moderate supersonic Mach numbers. The airplane had no horizontal tail assembly. The fineness ratio of the fuselage was 5.61, this low value being required to accommodate the proposed power units.

The wing plan form consisted of an equilateral triangle of aspect ratio 2.31. The profile at all spanwise stations was an

[redacted]

NACA 65-006.5 section. Longitudinal control was provided by constant-chord flaps extending from the fuselage to the wing tips. Flap deflections for the model were obtained by bending the rear portions of identical interchangeable wings to the positions desired.

Models with two types of air entries designed for the same power unit, were tested. The first was an external compression entry having a 50° cone at the entrance and a lip angle of 25° with the minimum cross-sectional area located at the entrance. (See fig. 2(a).) This entry is hereinafter referred to as the "external compression entry." The second entry was an open nose entry, the exterior profile being formed by fairing a truncated 24° cone into the cylindrical fuselage. The minimum duct area, as with the first entry, was also located at the entrance. (See fig. 2(b).) From the figure, it may be seen that the model with the open nose entry was tested with a cockpit canopy. For the model with the external compression entry, the cockpit was assumed to be located in the cone and inner body.

The various models were obtained by assembling interchangeable components on a basic inner body. The inner body, in turn, was attached to the end of a sting support which transmitted aerodynamic forces and pitching moments to the strain-gage balance. (See fig. 4.) Aerodynamic forces on the sting were minimized through the use of a shroud extending longitudinally to within 0.020 inch of the base of the inner body. This gap provided sufficient clearance between the inner body and the shroud to prevent mechanical interference resulting from deflection of the drag gage.

Variation in the angle of attack was accomplished by supporting the model successively on a series of bent stings. (See fig. 4.)

Lift, drag, and pitching moment were determined at angles of attack from −4° to 14° for Mach numbers from 0.5 to 0.95 and from 1.20 to 1.52. The corresponding Reynolds number variation is shown in figure 5. The decrease in Reynolds number at the higher subsonic Mach numbers and the apparently low values at supersonic Mach numbers resulted from increased tunnel operating temperatures.

The static pressure at the base of the inner body (necessary for determining base drag corrections) was measured through an orifice in the sting located adjacent to the base of the inner body as shown in figure 4. The pressures for determining internal flow conditions were obtained from a rake of six total-pressure and two static-pressure tubes mounted symmetrically about the perimeter of

[redacted]

the shroud in the jet exit. The shroud was attached to the balance housing in a manner which permitted concentric alinement of the shroud and rake with the sting and inner body, under load, at all angles of sting deflection.

REDUCTION OF DATA

The lift, drag, and pitching-moment coefficients are referred to the gross triangular wing area, including that portion covered by the fuselage. The pitching-moment coefficient is based upon the mean aerodynamic chord and referred to the quarter-chord position. Internal drag forces were calculated from pressure observations by use of momentum theory according to the method of reference 1; all other force data were obtained by direct measurement.

Conventional wind-tunnel-wall corrections at subsonic Mach numbers were determined by the method of reference 2. These corrections were:

$$\Delta\alpha = 0.724\ C_L$$

$$\Delta C_D = 0.0126\ C_L^2$$

A further correction, for constriction effects of the wind-tunnel walls at subsonic Mach numbers, was evaluated by the method of reference 3. At 0.95 Mach number this correction increased the measured values of Mach number and dynamic pressure by approximately 4 and 3 percent, respectively. Wall interference at supersonic Mach numbers was minimized by the model being almost entirely within the rhombus formed by the bow wave and its reflection from the side walls. No buoyancy corrections were applied to the drag data because of the small magnitude of the longitudinal pressure gradient present in the wind-tunnel air stream.

An adjustment to the measured drag forces was necessitated by the interference of the support. This interference varied with Mach number and was manifest as a change in pressure at the base of the inner body of the model from that value which would have existed if no support had been present. The variable drag resulting from this inconstant pressure was removed from the measured drag by correcting the values of the measured base pressure to correspond to that of the free stream.

[redacted]

RESULTS AND DISCUSSION

The relationships between lift, drag, and pitching-moment coefficients and angle of attack for the various model configurations are presented in figures 6, 7, and 8. The effects of Mach number on the static longitudinal stability, drag, and control effectiveness are shown in figures 9 through 13.

Static Longitudinal Stability

The static longitudinal stability of the model with external compression entry is indicated by the slope of the curve of the pitching-moment coefficient versus lift coefficient. (See fig. 6.) It is noted that the model is stable at all lift coefficients where trim is indicated and, in general, the stability increased with increase in Mach number.

The mass-flow coefficients of table I being sensibly the same for both air entries, it is concluded from a comparison of the pitching-moment curves of figure 8 that no change in the static longitudinal stability resulted from the change in type of air entry. This result should not be considered indicative of the effect of type of air entry upon airplane stability for other internal flow conditions.

The variation with Mach number of the position of the aerodynamic center of the model with either type of air entry, determined from the slope of the pitching-moment curves at zero lift coefficient in figure 8, is illustrated in figure 9. It is observed that the aerodynamic center lies somewhat aft of the centroid of gross wing area (50 percent of the mean aerodynamic chord) at Mach numbers above 1.27. This result is in sensible agreement with the results of an analytical study (reference 4) of the center of pressure of triangular wings in combination with various size bodies. In the reference paper, a center-of-pressure location of 59 percent of the mean aerodynamic chord was predicted for the ratio of body diameter to wing span of the present investigation.

The variation of the aerodynamic center of the model with Mach number agrees well with that shown on figure 9 for a thin wing of similar plan form at subsonic Mach numbers and at a Reynolds number of 5.3×10^6. (See reference 5.)

[redacted]

Drag Characteristics

It is emphasized at the outset that the absolute values of the drag coefficient contained in this report are not directly applicable to the full-scale airplane, partly because in the tests no attempt was made to simulate the internal flow of the prototype. Drag values more characteristic of the airplane may be obtained by substituting for the measured internal drag coefficients of the model values more representative of those prevailing for the actual airplane. For further comparison with the full-scale aircraft, values of the model mass-flow coefficient are given in table I. The variations of minimum drag coefficient with Mach number for the body, body plus wing, and body plus wing plus vertical fin of the model with external compression entry are shown in figure 10. For the complete configuration, the variation of minimum drag coefficient with Mach number is characteristic of that previously observed for triangular wings of aspect ratio 2. (See reference 6.) The minimum drag coefficient displayed little variation with Mach number either below 0.85 or above 1.20 Mach number and indicated an increase of approximately 100 percent between these Mach numbers.

It is further evident from figure 10 that the fuselage contributes from about 60 percent, at subsonic Mach numbers, to about 80 percent, at supersonic Mach numbers, to the total minimum drag coefficient of the test model. A large portion of this high fuselage drag, in some instances more than 50 percent, was found to consist of the internal drag of the model. Results of the internal drag measurements are shown in figure 11. The internal drag coefficients shown are, for low and moderate lift coefficients, independent of the angle of attack. Although the internal flow remained subsonic at stream Mach numbers of 1.20 and 1.27, the scatter of the data at these Mach numbers indicates that the measurements are somewhat unreliable. They have been presented, however, to indicate the order of magnitude of the internal drag.

Comparison of the minimum drag coefficients of the models equipped with the two types of air entry (fig. 12) shows that the use of the open nose entry reduced the minimum drag coefficient of the model at all Mach numbers. The reduction was particularly substantial at supersonic Mach numbers, although with increasing supersonic Mach number the advantage diminished. This result should not be interpreted to mean that the open nose type of air entry is necessarily superior to the external compression type. The evidence of reference 7 indicates that the external compression entry of the present investigation was functioning improperly at least at 1.5 Mach number in that the entry shock was not swallowed, with the result that the flow over the exterior of the model was adversely affected.

[redacted]

Control Effectiveness

The effects of various angles of control-surface deflection on the lift, drag, and pitching-moment characteristics of the model with the external compression entry are shown in figure 6. The respective variations with Mach number of the average rate of change of lift coefficient and pitching-moment coefficient with control-surface deflection from 0° to 10° derived from these curves are given in figure 13. Also shown are the corresponding characteristics at a Mach number of 1.53 determined from tests of the same model (reference 7) at a comparable Reynolds number.

The variation with Mach number of lift effectiveness was small at subsonic Mach numbers. At supersonic Mach numbers, the lift effectiveness averaged approximately 50 percent of the subsonic value.

The pitching-moment effectiveness of the control surface exhibited a small increase with increasing subsonic Mach number and a continuous decrease with increasing supersonic Mach number to a value at 1.5 Mach number approximately 50 percent of the subsonic value.

A comparison of the control effectiveness determined in this investigation with that reported in reference 5 for a thin wing of similar plan form at 5.3×10^6 Reynolds number is made in figure 13. The close correspondence of these results indicates that a Reynolds number variation within the limits of the respective tests exerts little influence on the model control effectiveness.

CONCLUSIONS

From the results of a wind-tunnel investigation between 0.50 and 1.52 Mach number to determine the variation with Mach number of the static longitudinal stability, the drag, and the effectiveness of a constant-chord control surface for a model of a tailless fighter aircraft employing a wing of triangular plan form and provided with two alternate types of air entry, it is concluded:

1. The static longitudinal stability of the model, referred to the quarter point of the mean aerodynamic chord, increased continuously with Mach number throughout the range of the investigation where trim was indicated. The stability was not appreciably affected by the type of air entry employed.

2. The variation with Mach number of the minimum drag coefficient was characteristic of triangular wings of similar aspect ratio.

[redacted]

3. The minimum drag coefficient of the model with the open nose air entry was lower at all Mach numbers, and substantially lower at supersonic Mach numbers, than that of the configuration with the external compression entry.

4. The variation with subsonic Mach numbers of the lift and pitching-moment effectiveness of the constant-chord trailing-edge flap was small. At supersonic Mach numbers, the lift effectiveness was approximately 50 percent of the subsonic value. The pitching-moment effectiveness at supersonic Mach numbers decreased continuously from the maximum subsonic value to half of this value at 1.52 Mach number.

Ames Aeronautical Laboratory,
National Advisory Committee for Aeronautics,
Moffett Field, Calif.

REFERENCES

1. Becker, John V., and Baals, Donald D.: The Aerodynamic Effects of Heat and Compressibility in the Internal Flow Systems of Aircraft. NACA Rep. No. 773, 1943.

2. Glauert, H.: Wind Tunnel Interference on Wings, Bodies, and Air Screws. British R & M No. 1566, Sept. 1933.

3. Herriot, John G.: Blockage Corrections for Three-Dimensional-Flow Closed-Throat Wind Tunnels with Consideration of the Effect of Compressibility. NACA RM No. A7B28, 1947.

4. Sprieter, John R.: Aerodynamic Properties of Slender Wing-Body Combinations at Subsonic, Transonic, and Supersonic Speeds. NACA TN No. 1662, 1948.

5. Stephenson, Jack D., and Amuedo, Arthur R.: Tests of a Triangular Wing of Aspect Ratio 2 in the Ames 12-foot Pressure Tunnel. II - The Effectiveness and Hinge Moments of a Constant-Chord Plain Flap. NACA RM No. A8E03, 1948.

6. Berggren, Robert E., and Summers, James L.: Aerodynamic Characteristics at Subsonic and Supersonic Mach Numbers of a Thin Triangular Wing of Aspect Ratio 2. I - Maximum Thickness at 20 Percent of the Chord. NACA RM No. A8I16, 1948.

[redacted]

7. Scherrer, Richard, and Wimbrow, William R.: Wind-Tunnel Investigation at a Mach Number of 1.53 of an Airplane with a Triangular Wing. NACA RM No. A7J05, 1948.

[redacted]

TABLE I

VALUES OF MASS-FLOW COEFFICIENT

Mach number	Mass-flow coefficient, $\frac{m_1}{m_0}$	
	External compression entry	Open nose entry
0.5	0.87	0.95
.6	.87	.94
.7	.84	.91
.8	.79	.87
.9	.77	.84
.95	.77	.84
1.20	.86	1.00
1.27	.82	.86

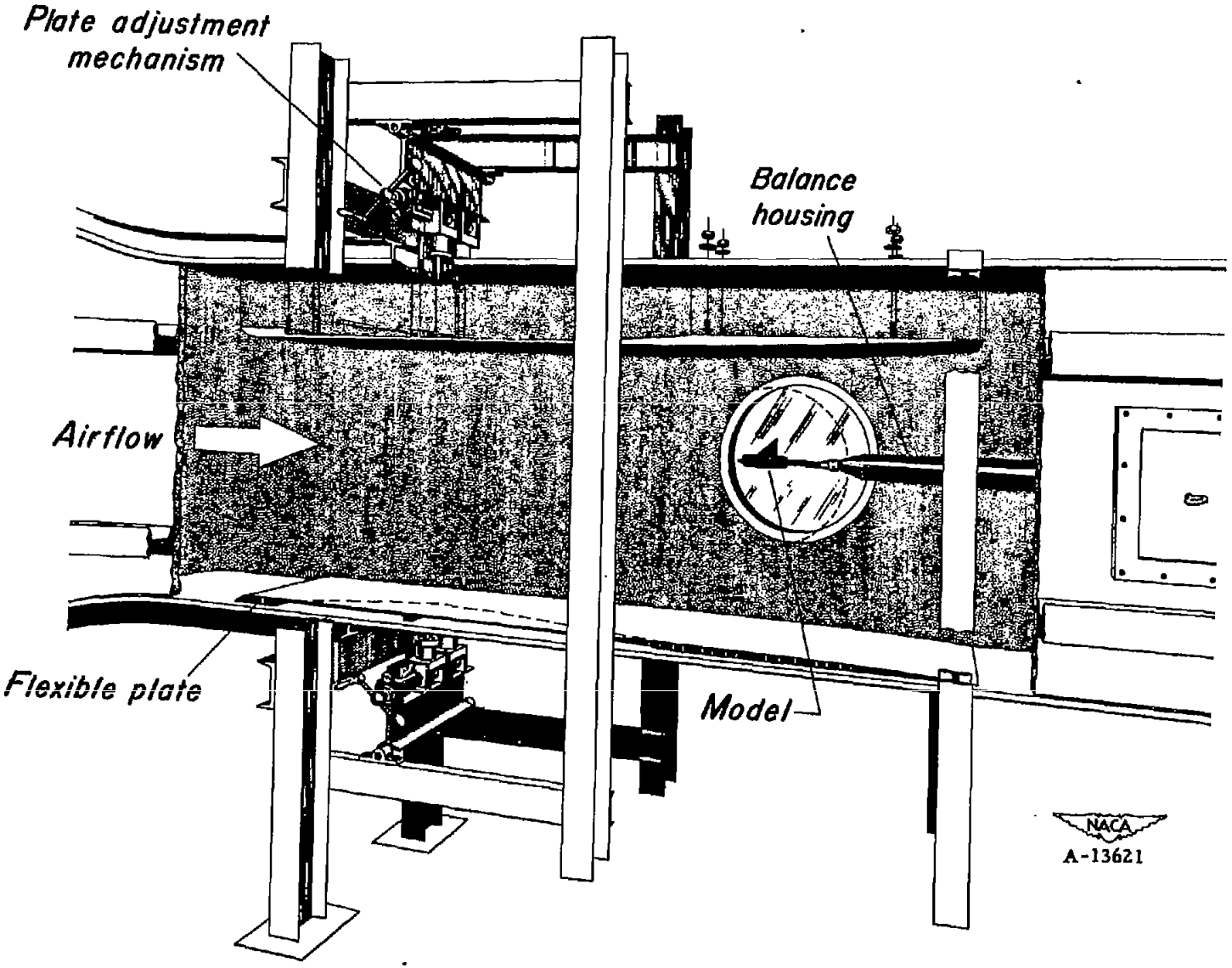

Figure 1.– Sectional drawing of flexible nozzle in the Ames 1– by 3-1/2–foot high–speed wind tunnel.

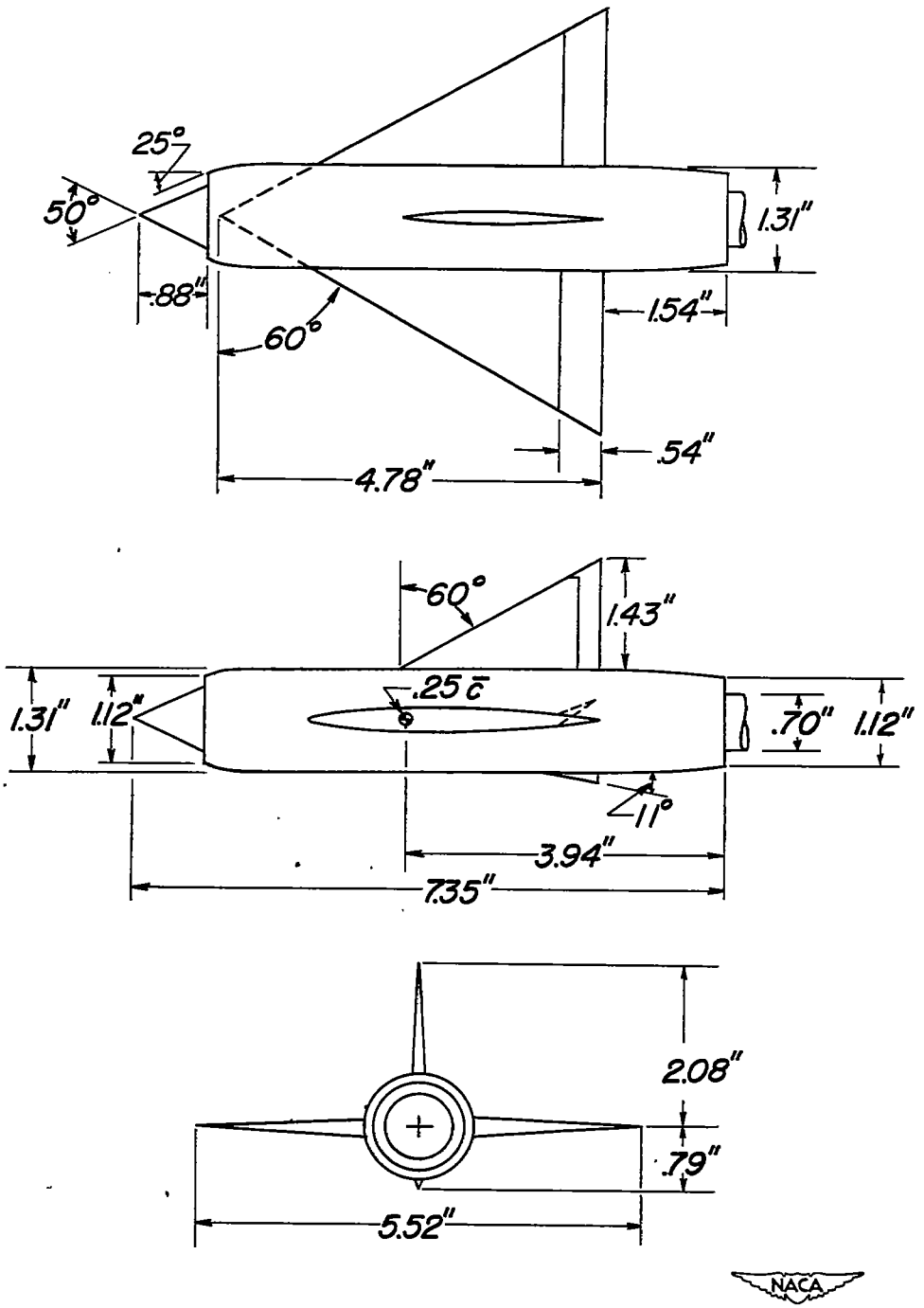

(a) External compression entry.

Figure 2.- Three-view drawing of models.

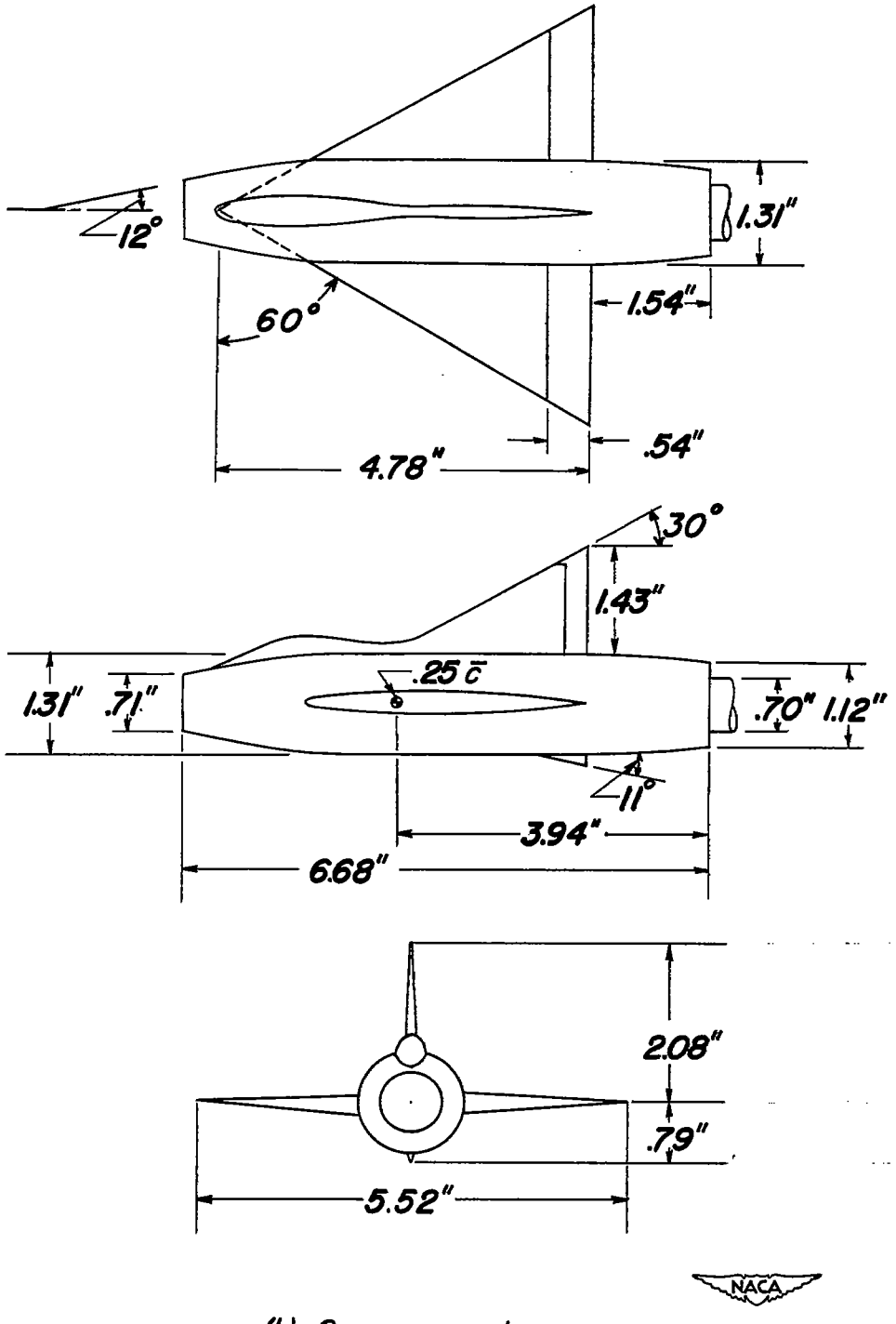

(b) Open nose entry.

Figure 2.- Concluded.

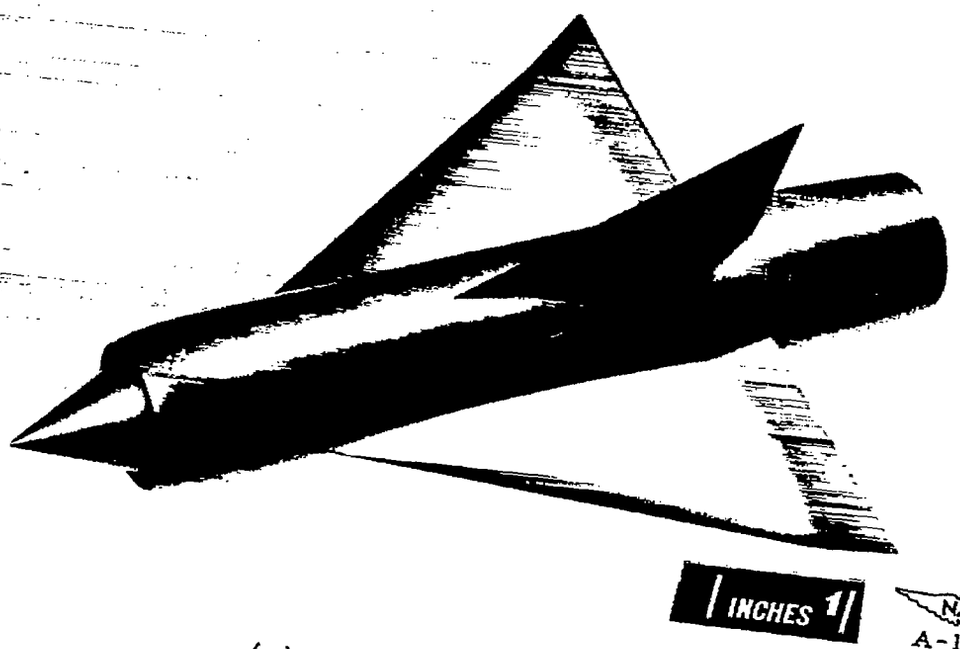

(a) External compression entry.

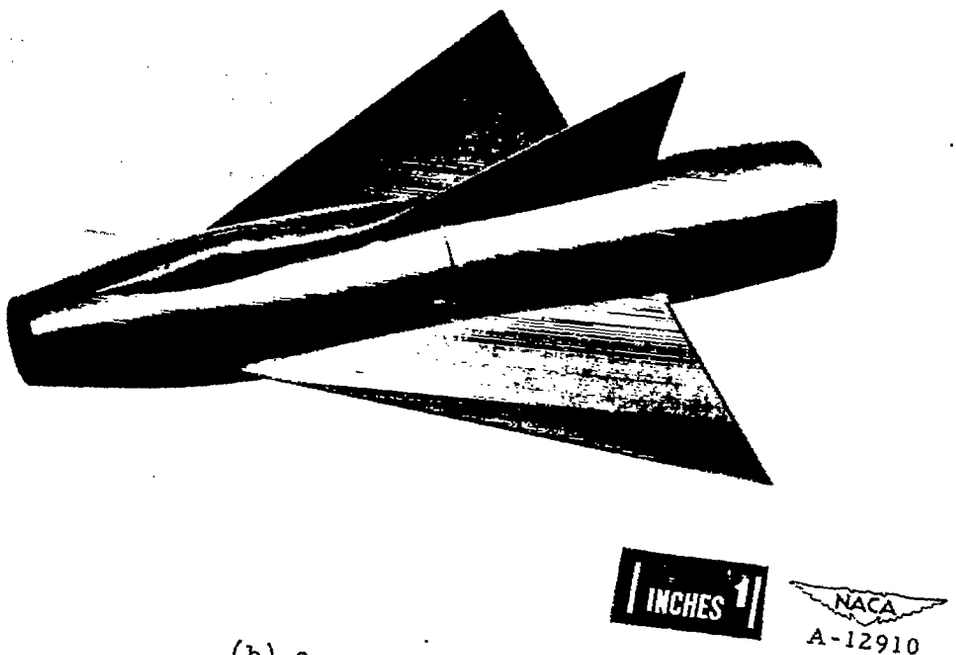

(b) Open nose entry.

Figure 3.- Photographs of models.

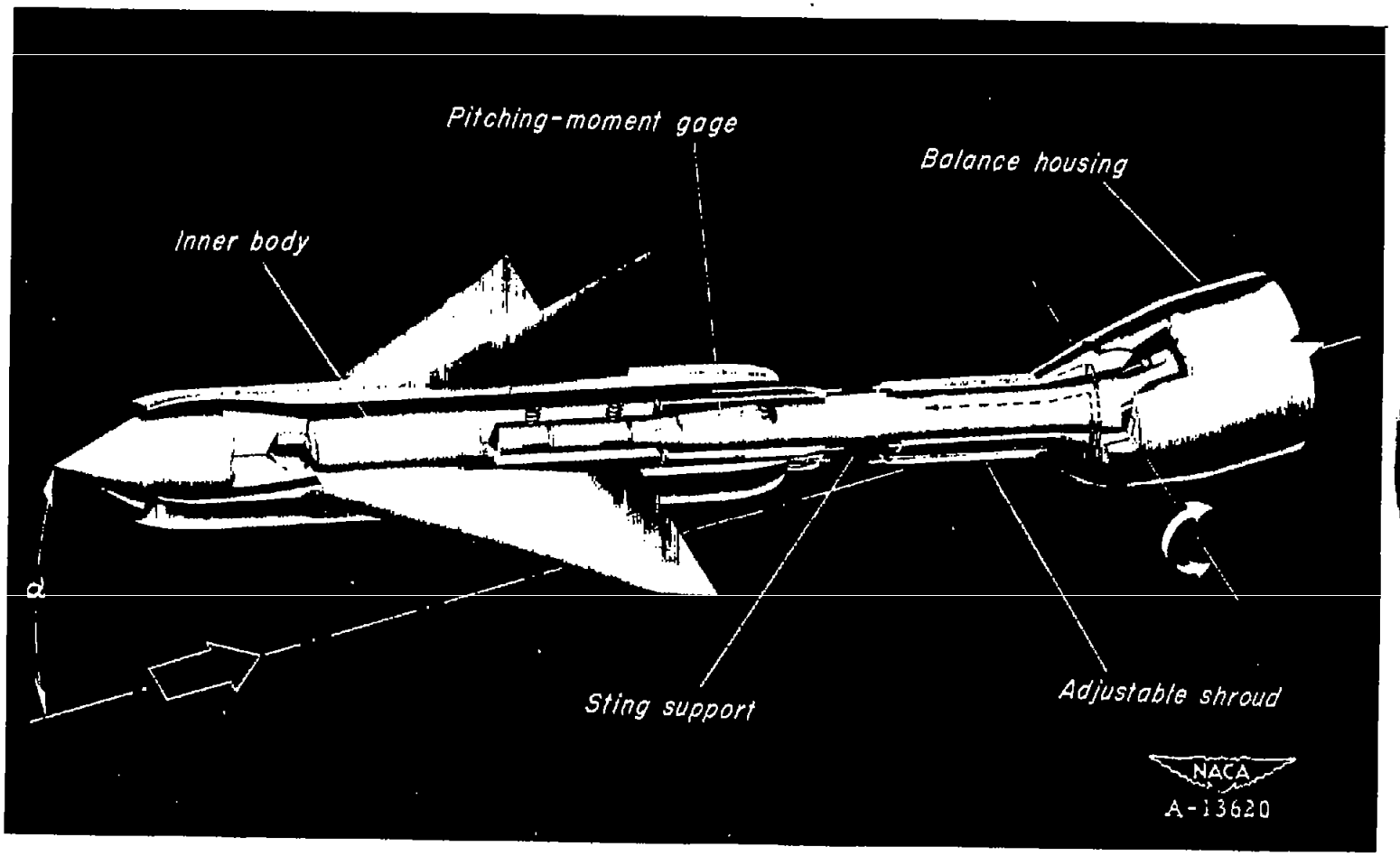

Figure 4.— Sectional view of model and support.

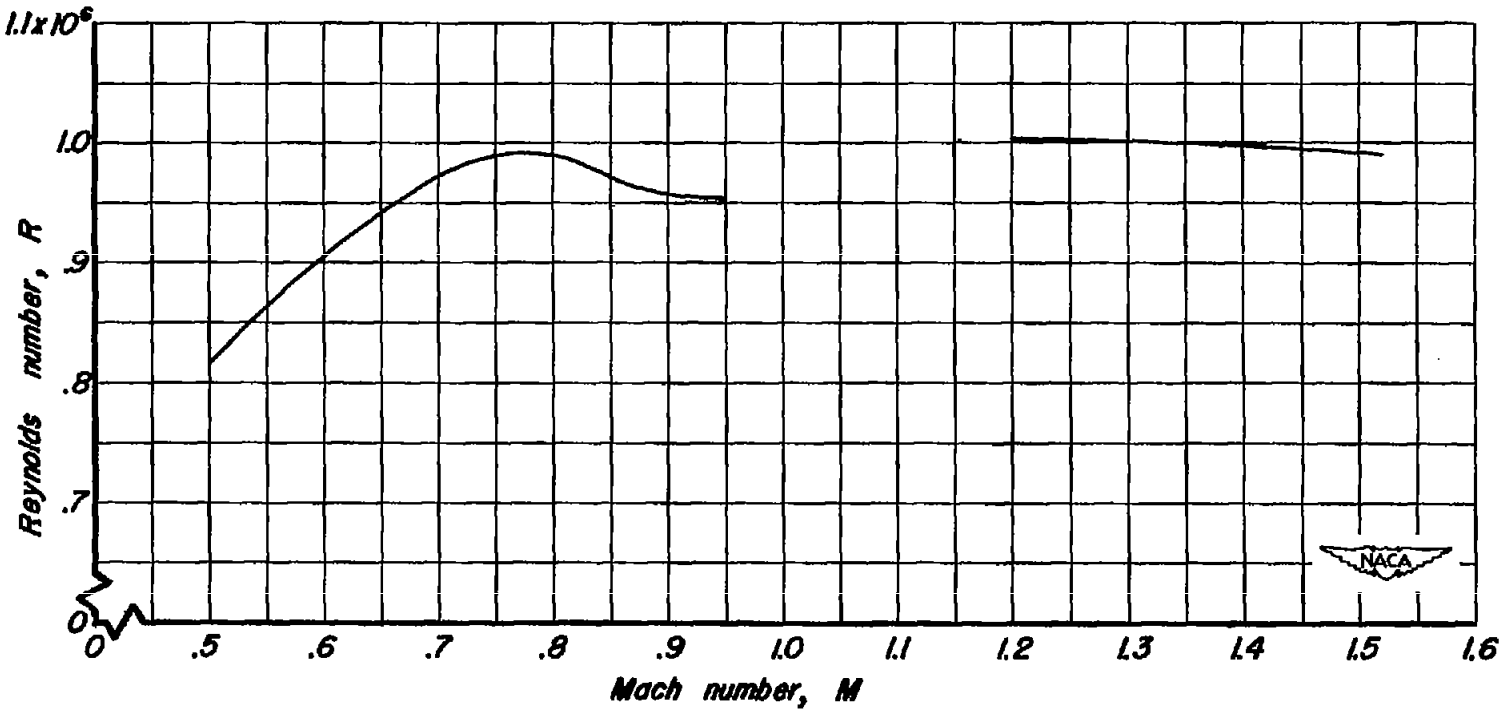

Figure 5.- Variation of Reynolds number with Mach number for the models in the Ames 1-by 3½-foot high-speed wind tunnel.

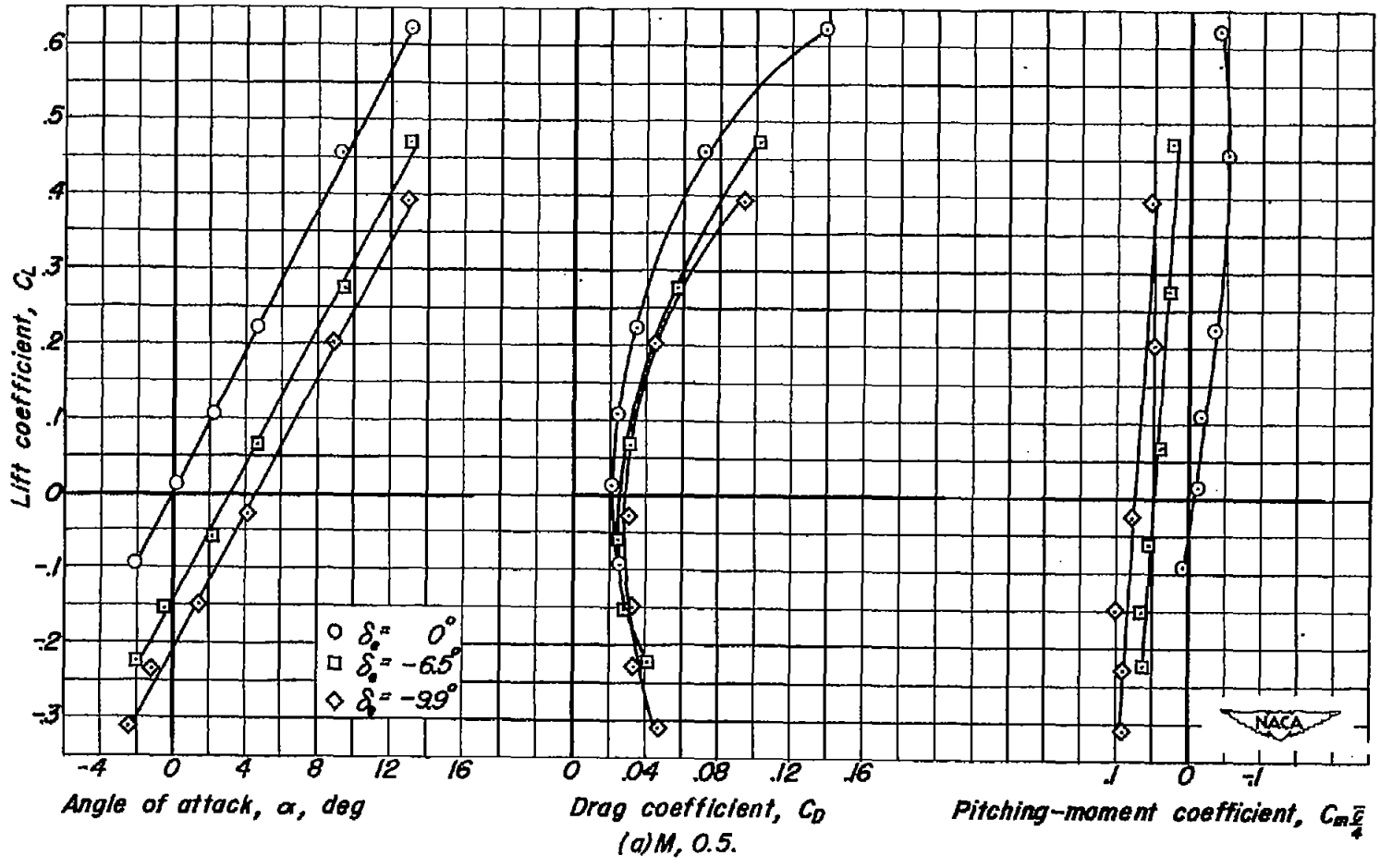

(a) M, 0.5.

Figure 6.–Variation of the aerodynamic characteristics for various flap deflections of the model with the external compression entry.

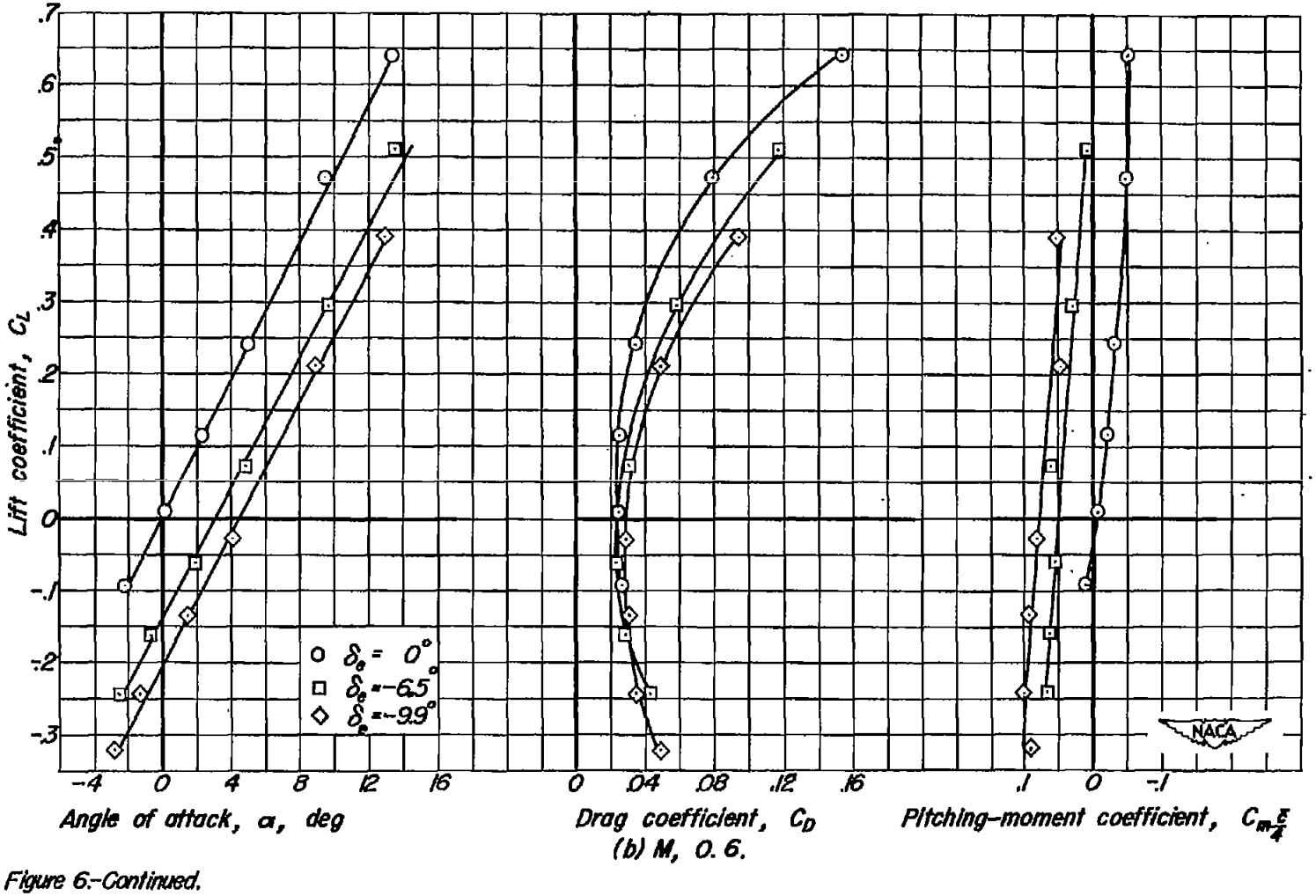

(b) M, 0.6.

Figure 6.-Continued.

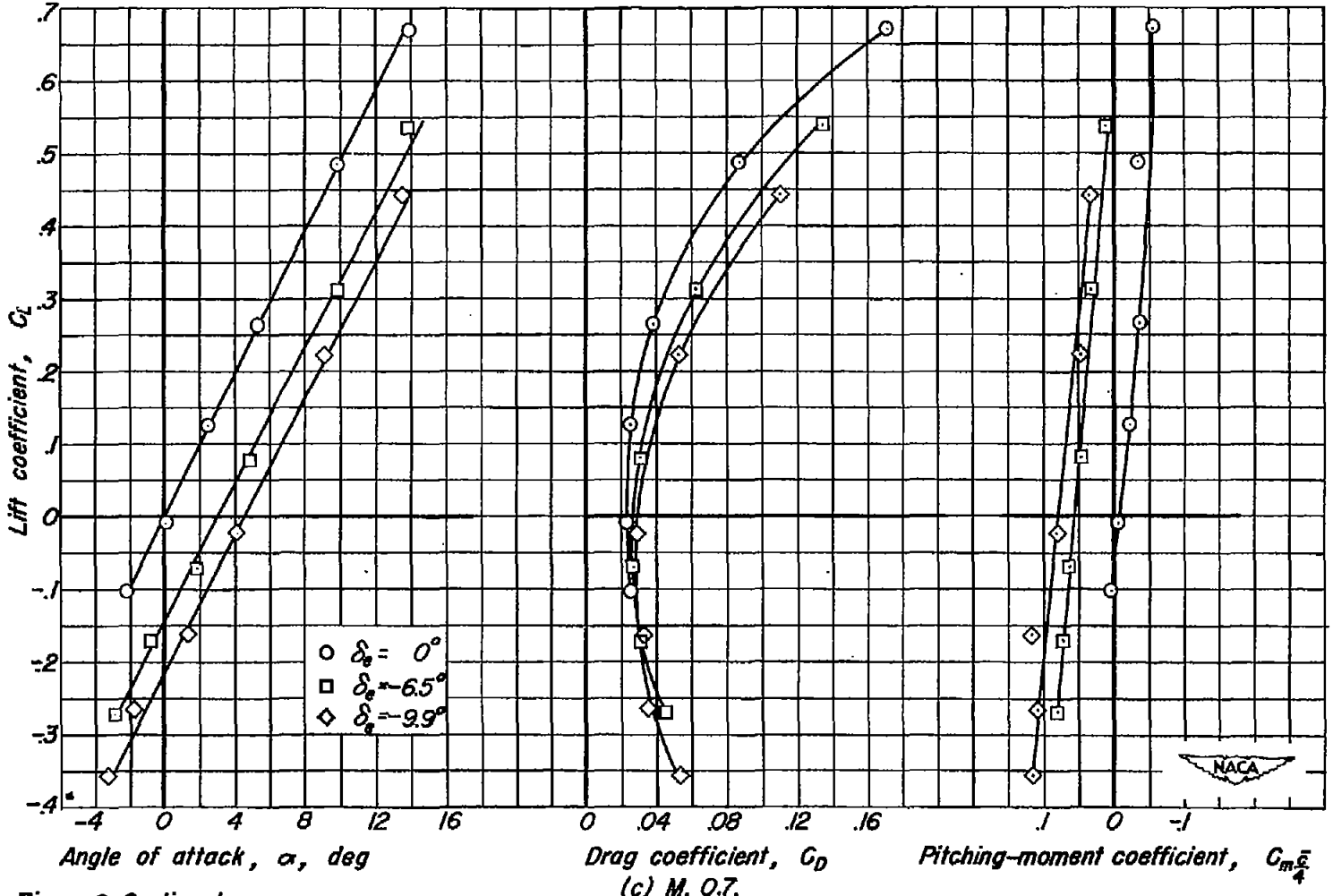

Figure 6.-Continued.

(c) M, 0.7.

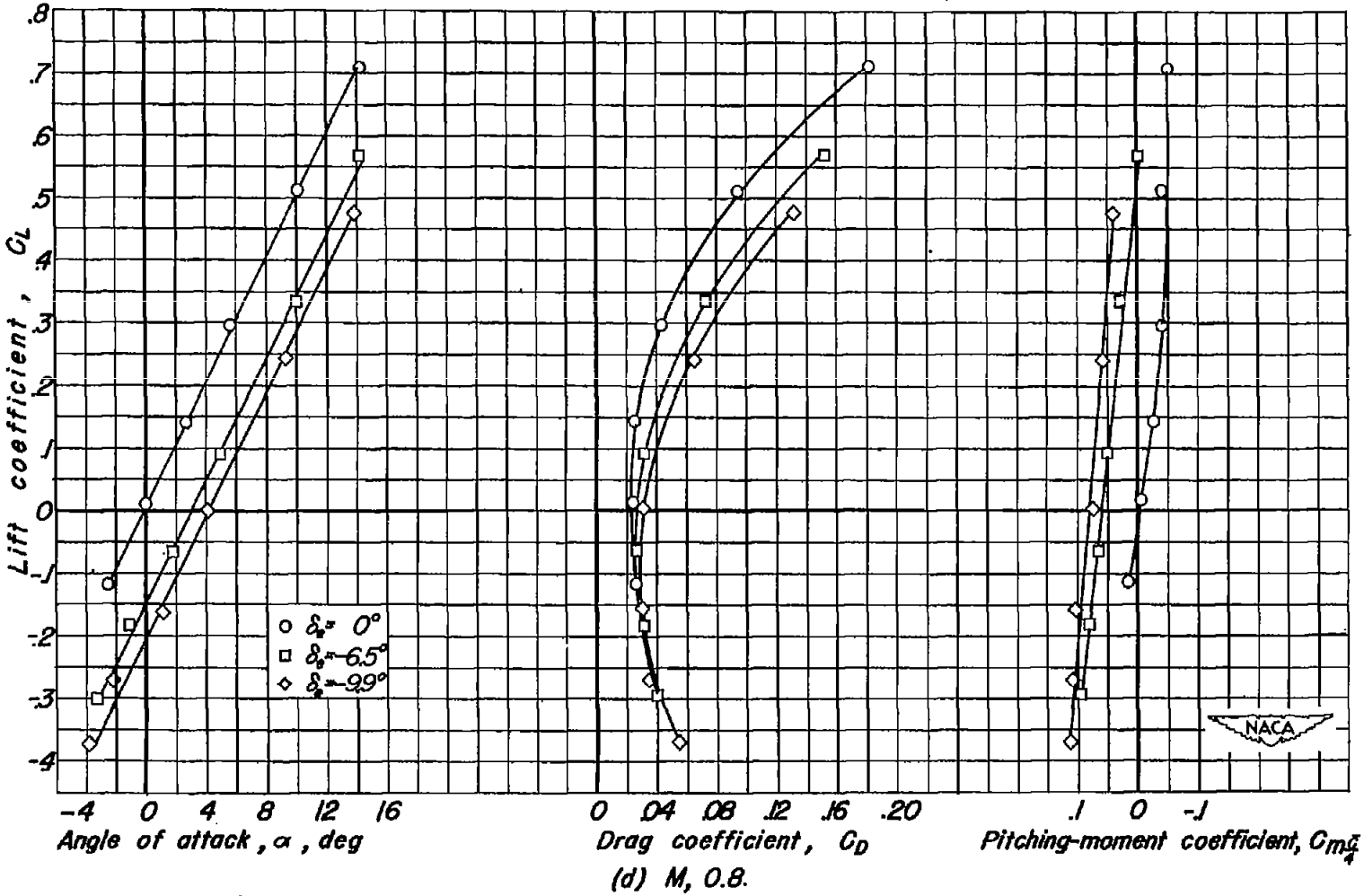

(d) M, 0.8.

Figure 6.-Continued.

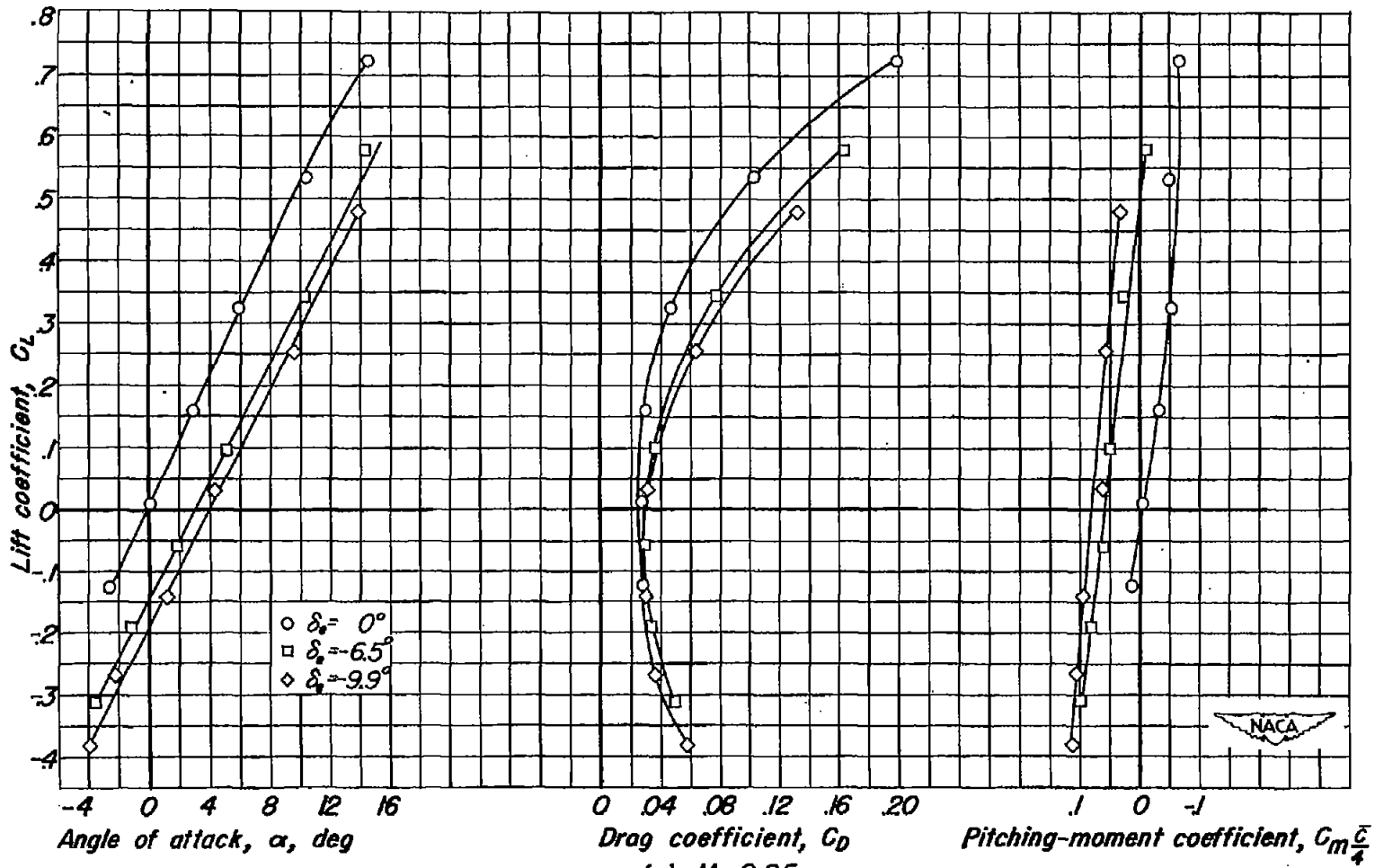

(e) M, 0.85.

Figure 6.-Continued.

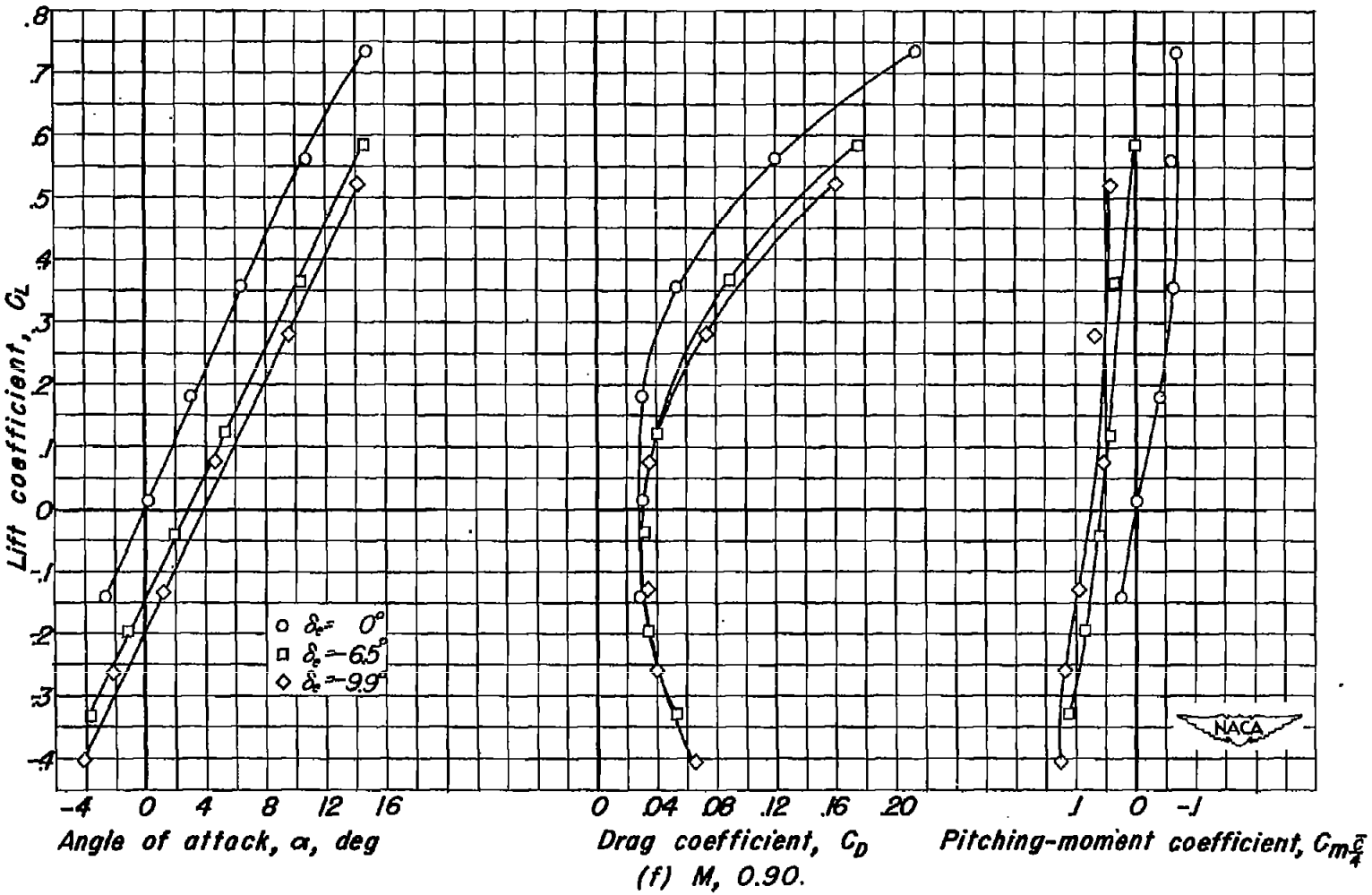

(f) M, 0.90.

Figure 6.-Continued.

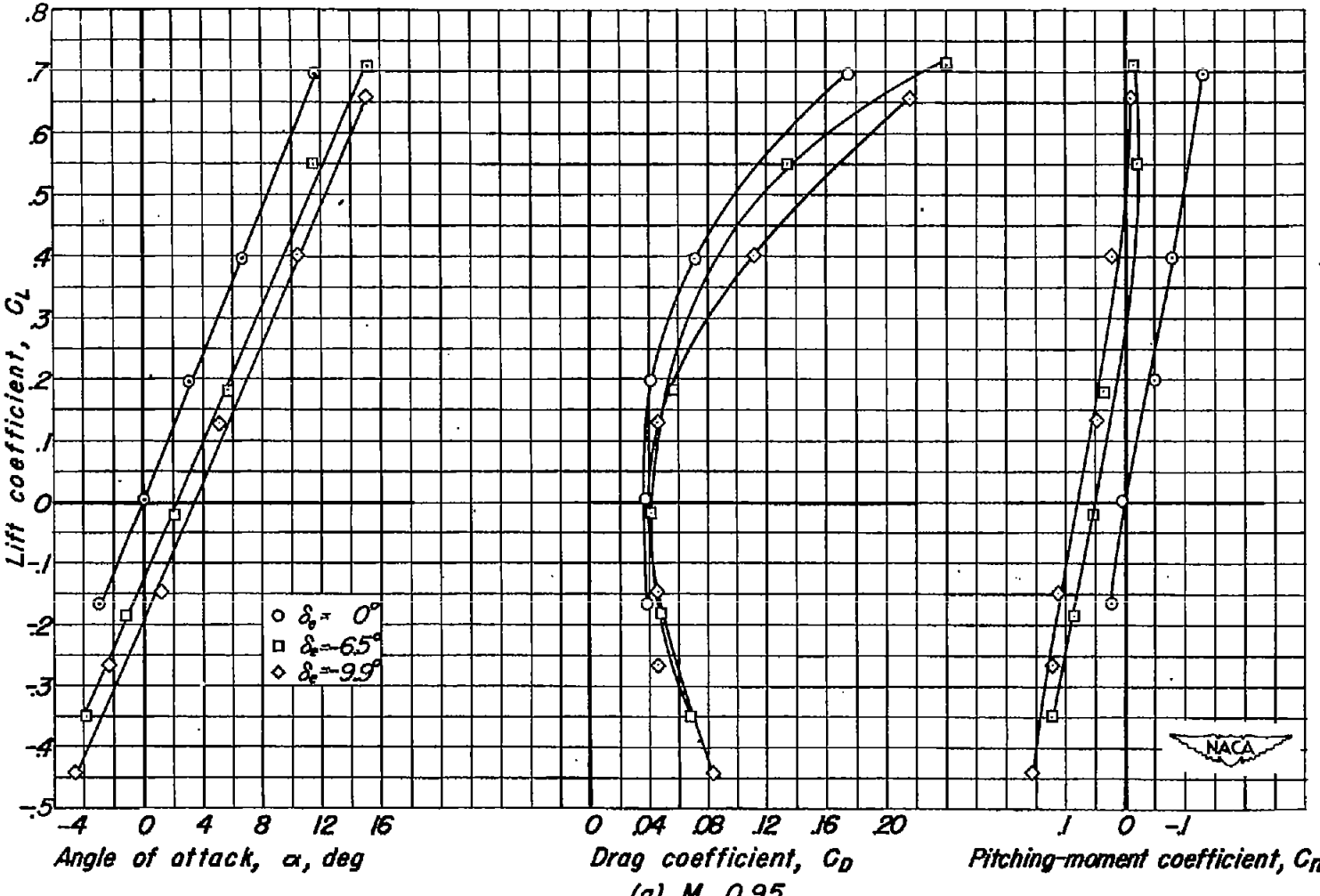

(g) M, 0.95.

Figure 6.-Continued.

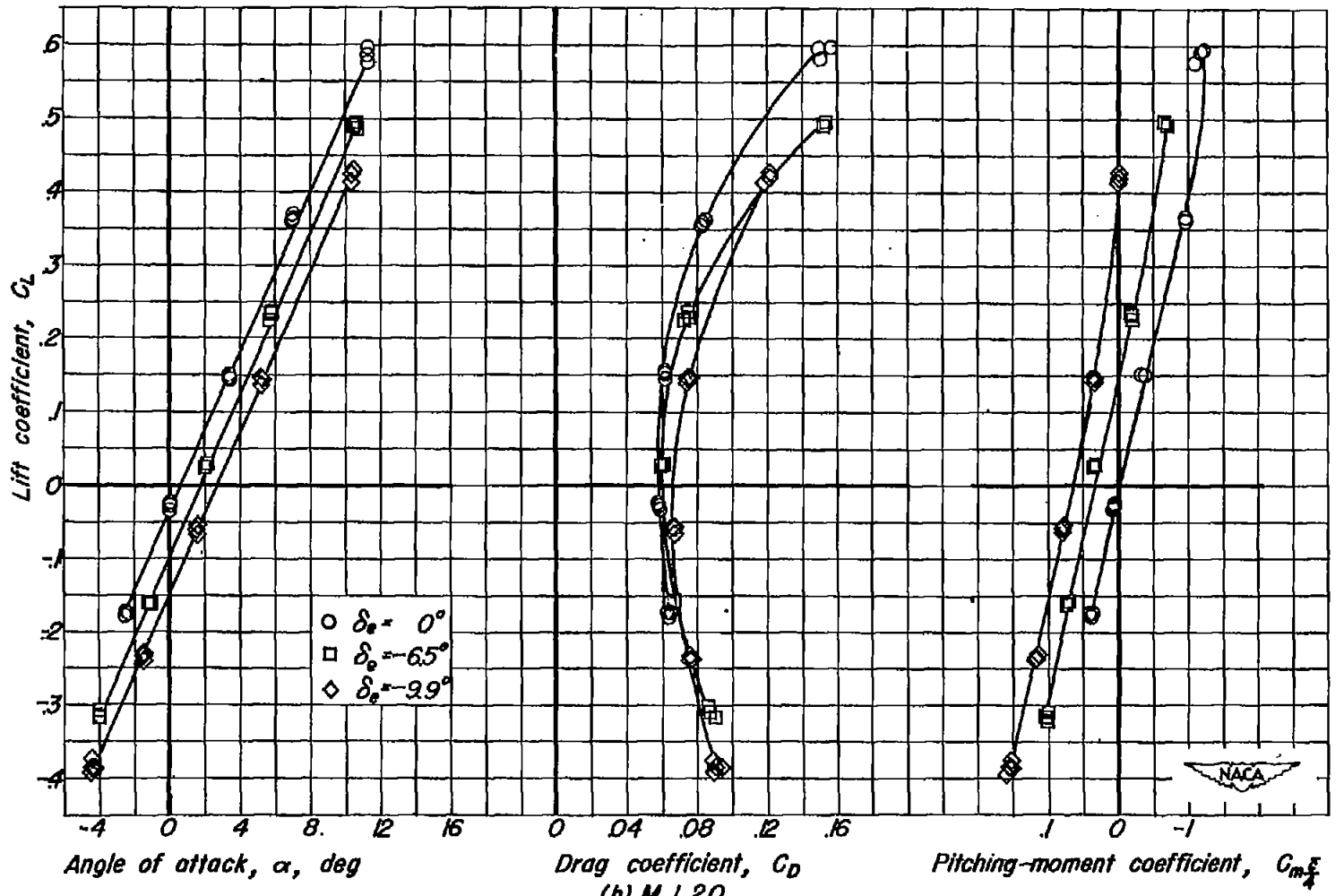

Figure 6.-Continued.

(h) M, 1.20.

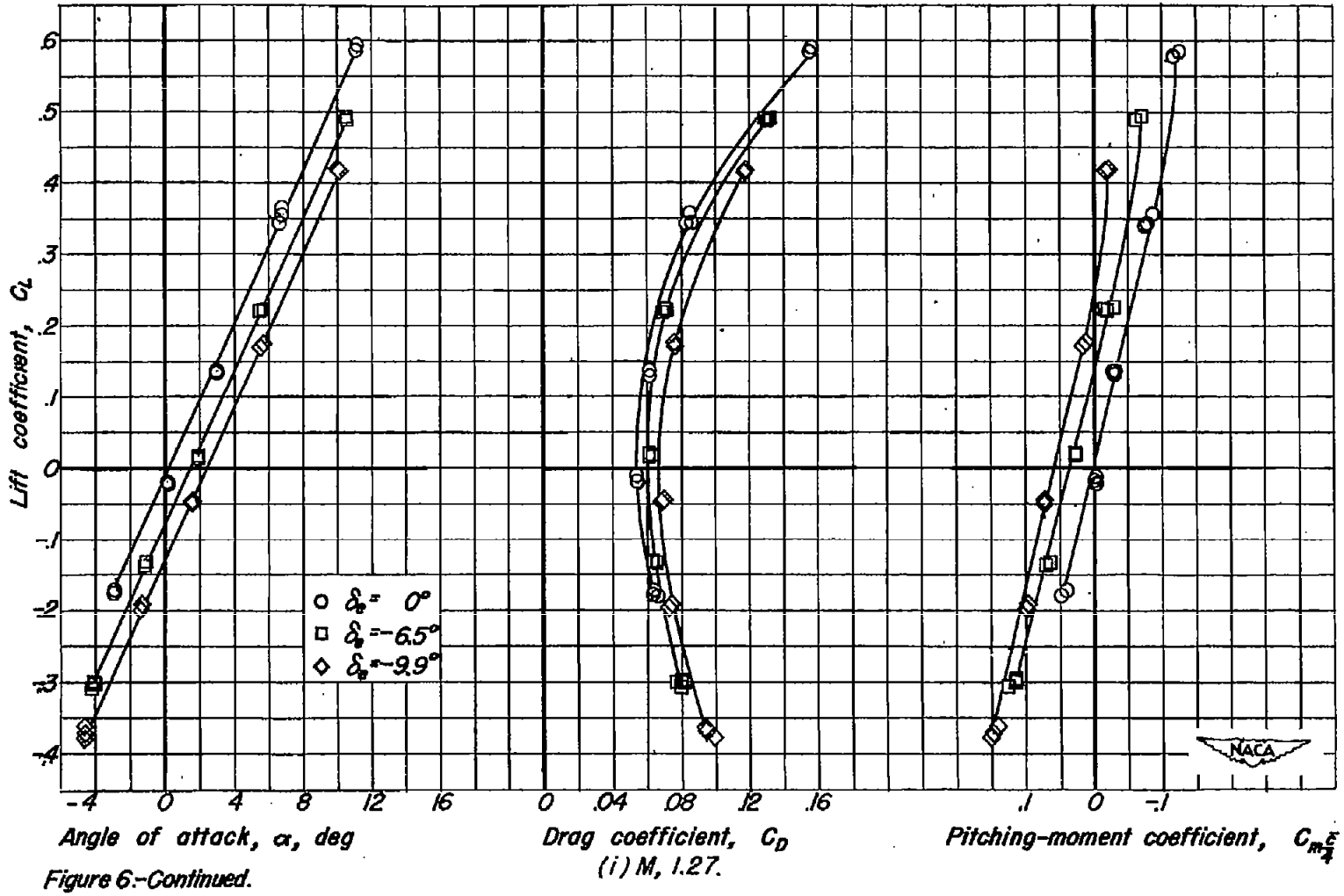

Figure 6.-Continued.

(i) M, 1.27.

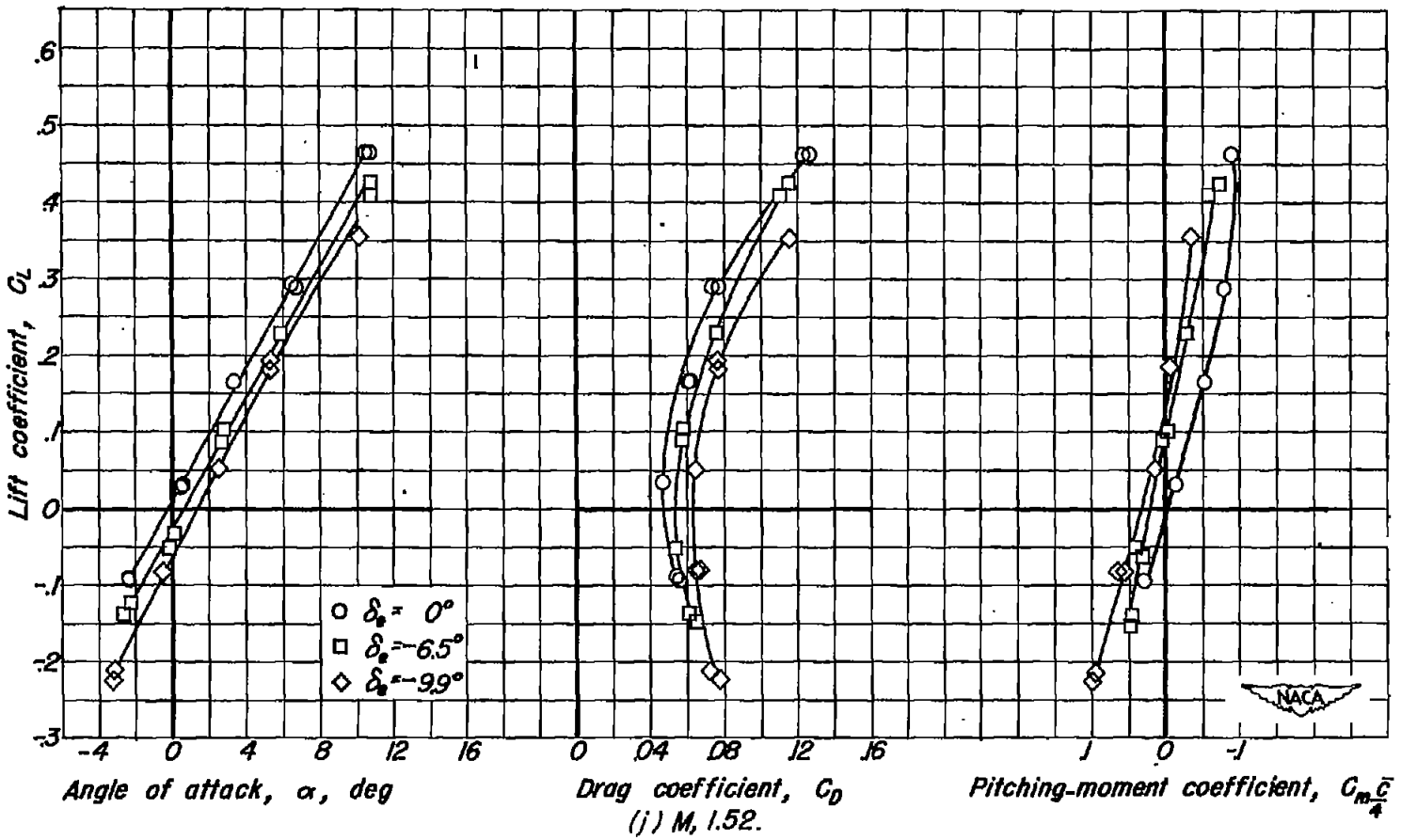

(j) M, 1.52.

Figure 6.-Concluded.

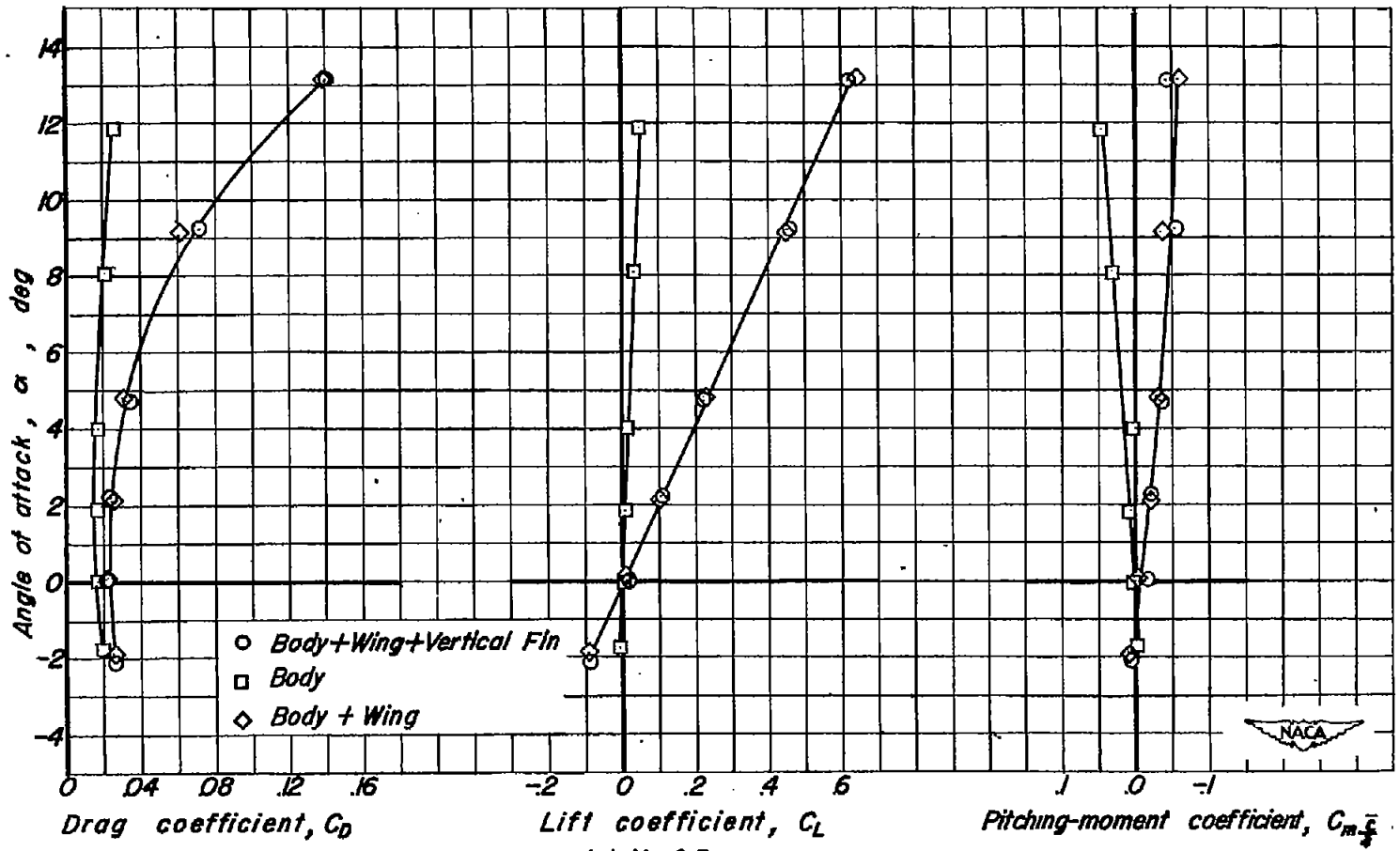

(a) M, 0.5.

Figure 7.–Variation of the aerodynamic characteristics of components of the model with the external compression entry.

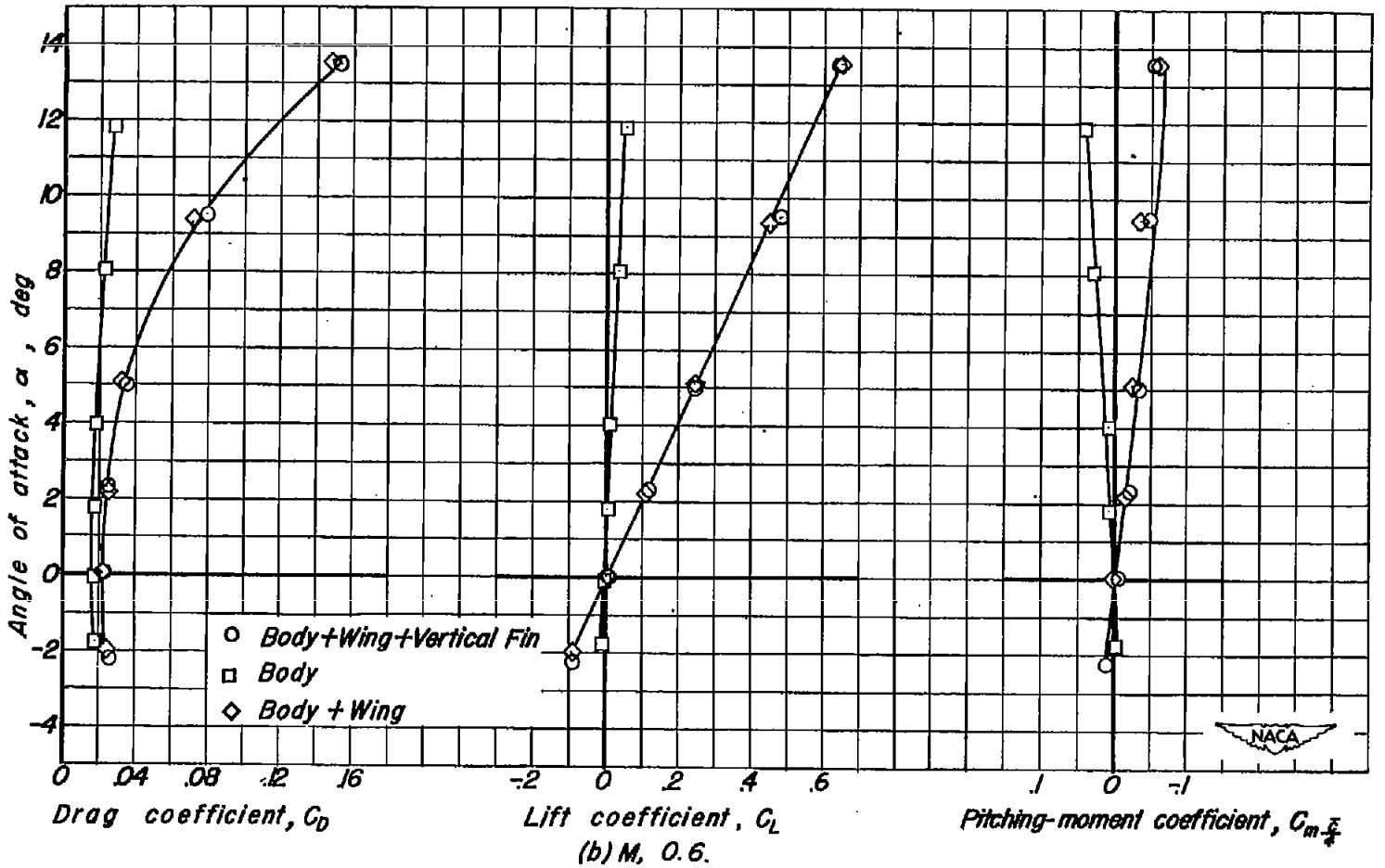

(b) M, 0.6.

Figure 7.-Continued.

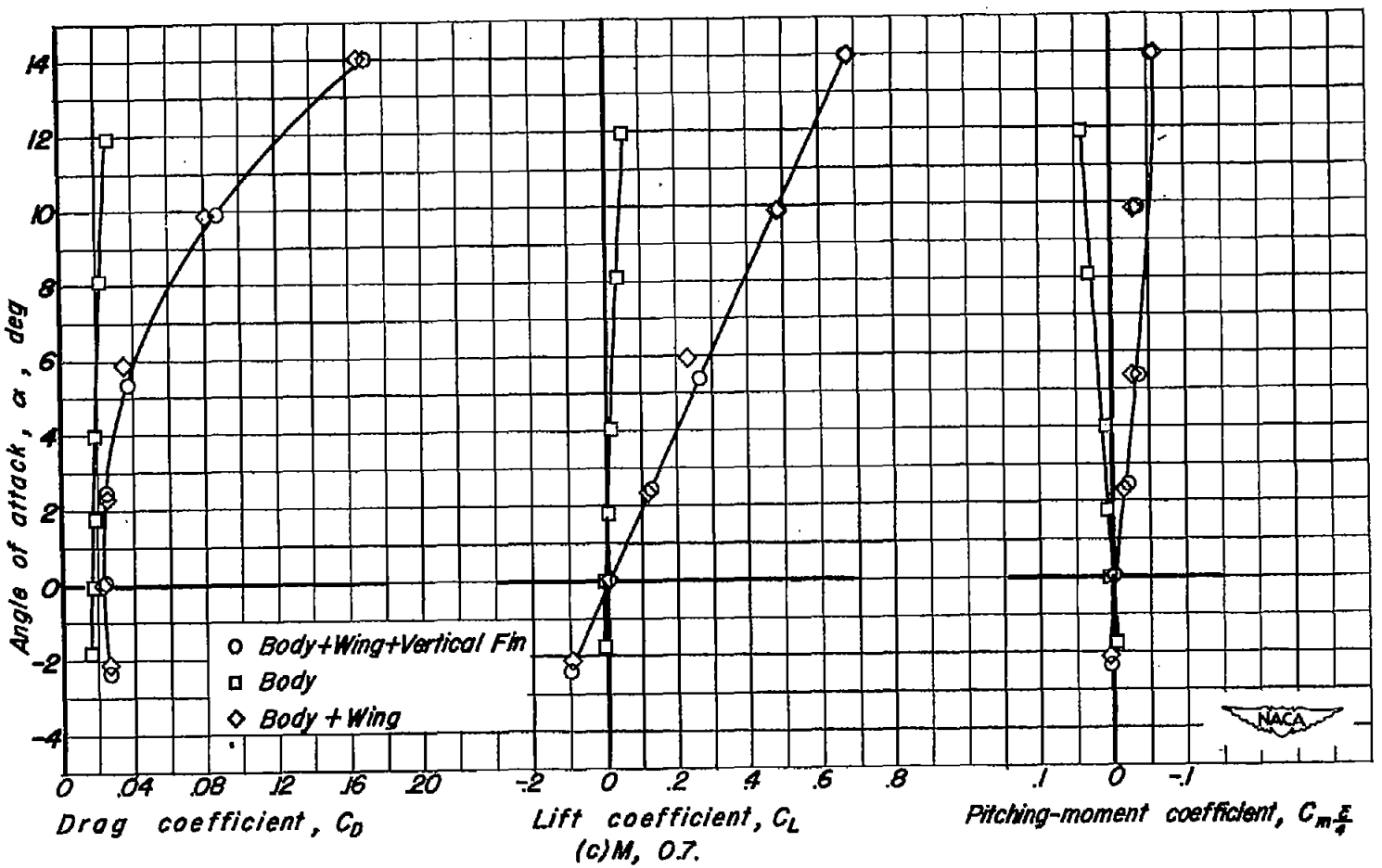

Figure 7.-Continued.

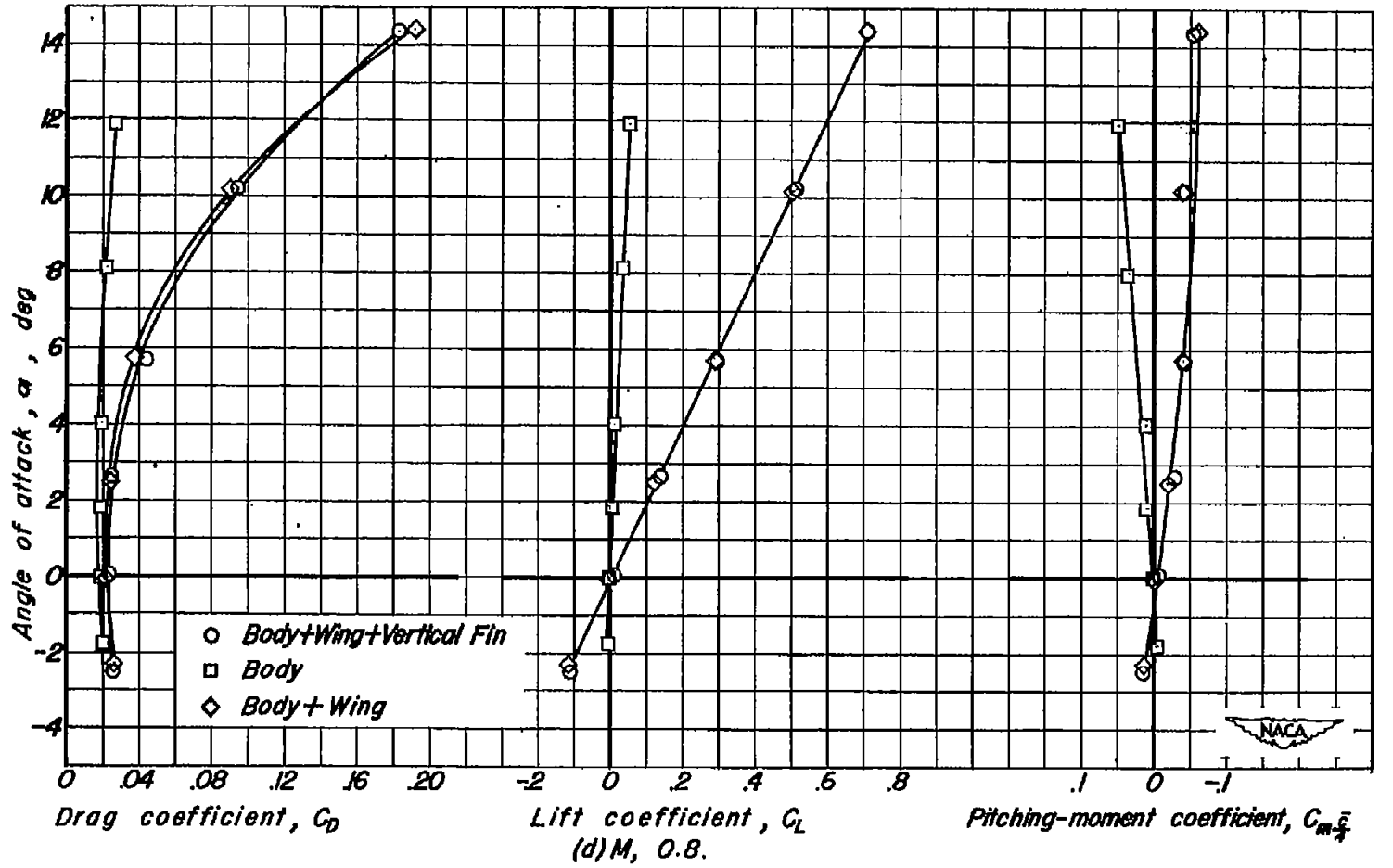

(d) M, 0.8.

Figure 7.-Continued.

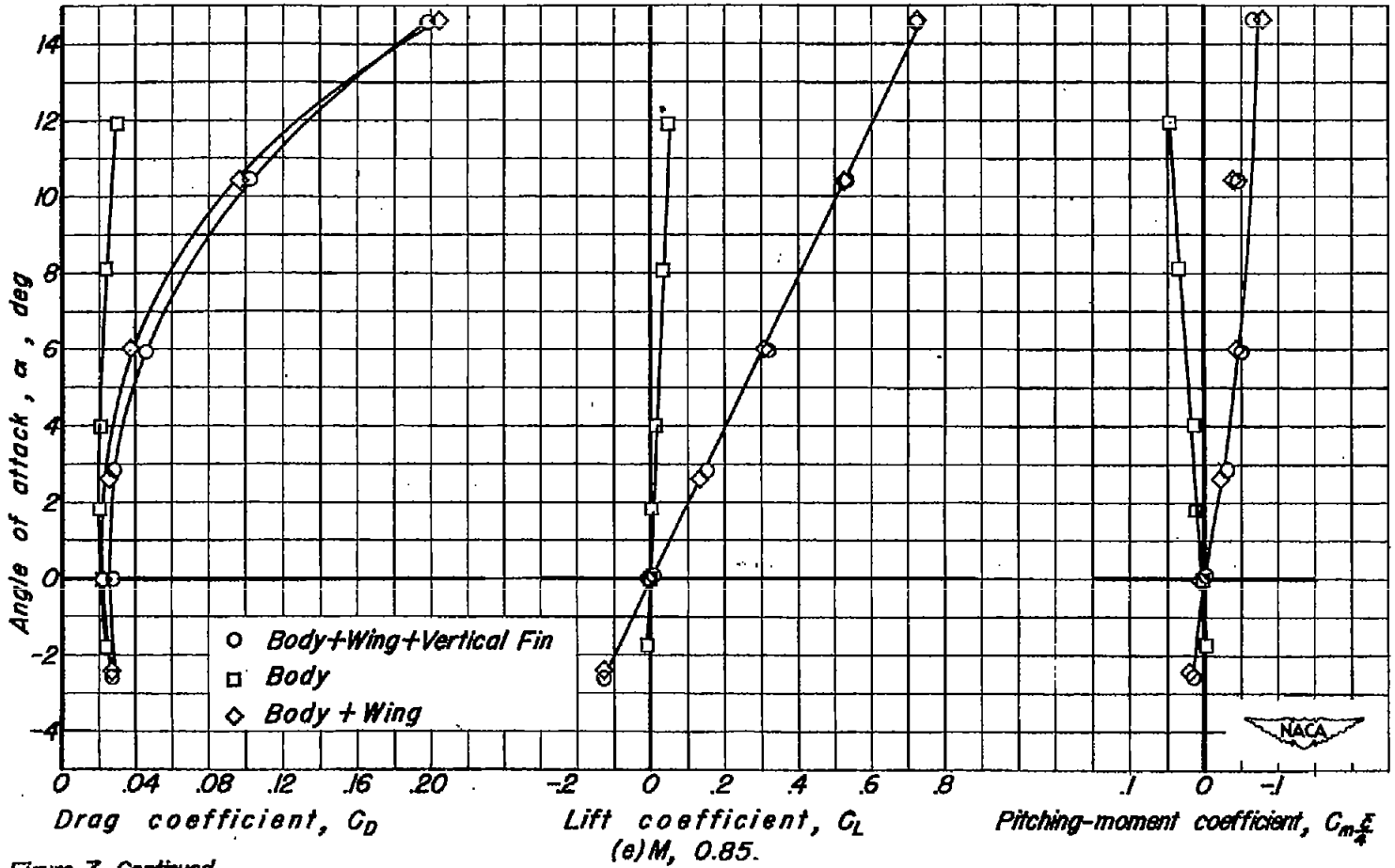

(e) M, 0.85.

Figure 7.-Continued.

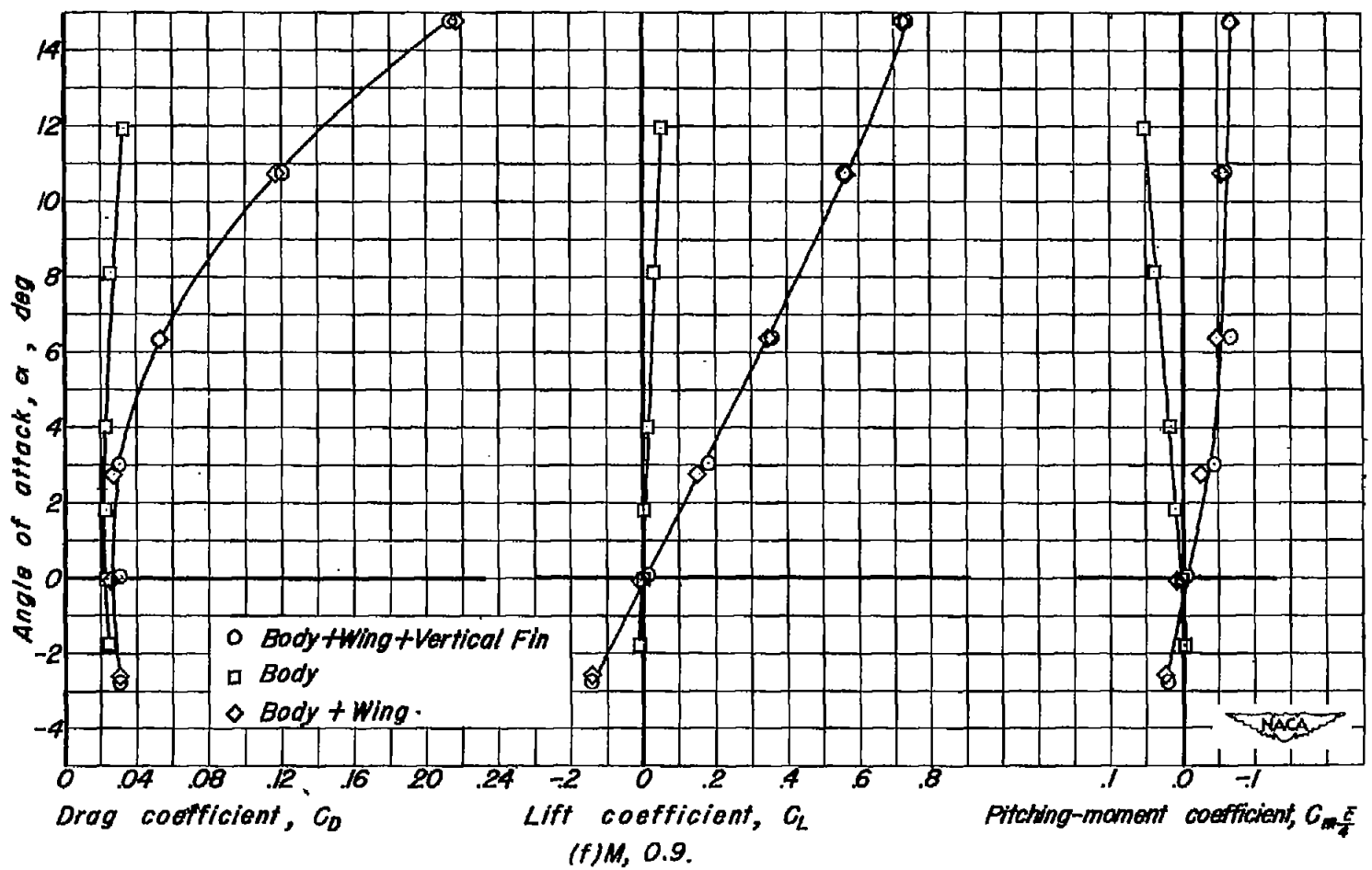

(f)M, 0.9.

Figure 7.-Continued.

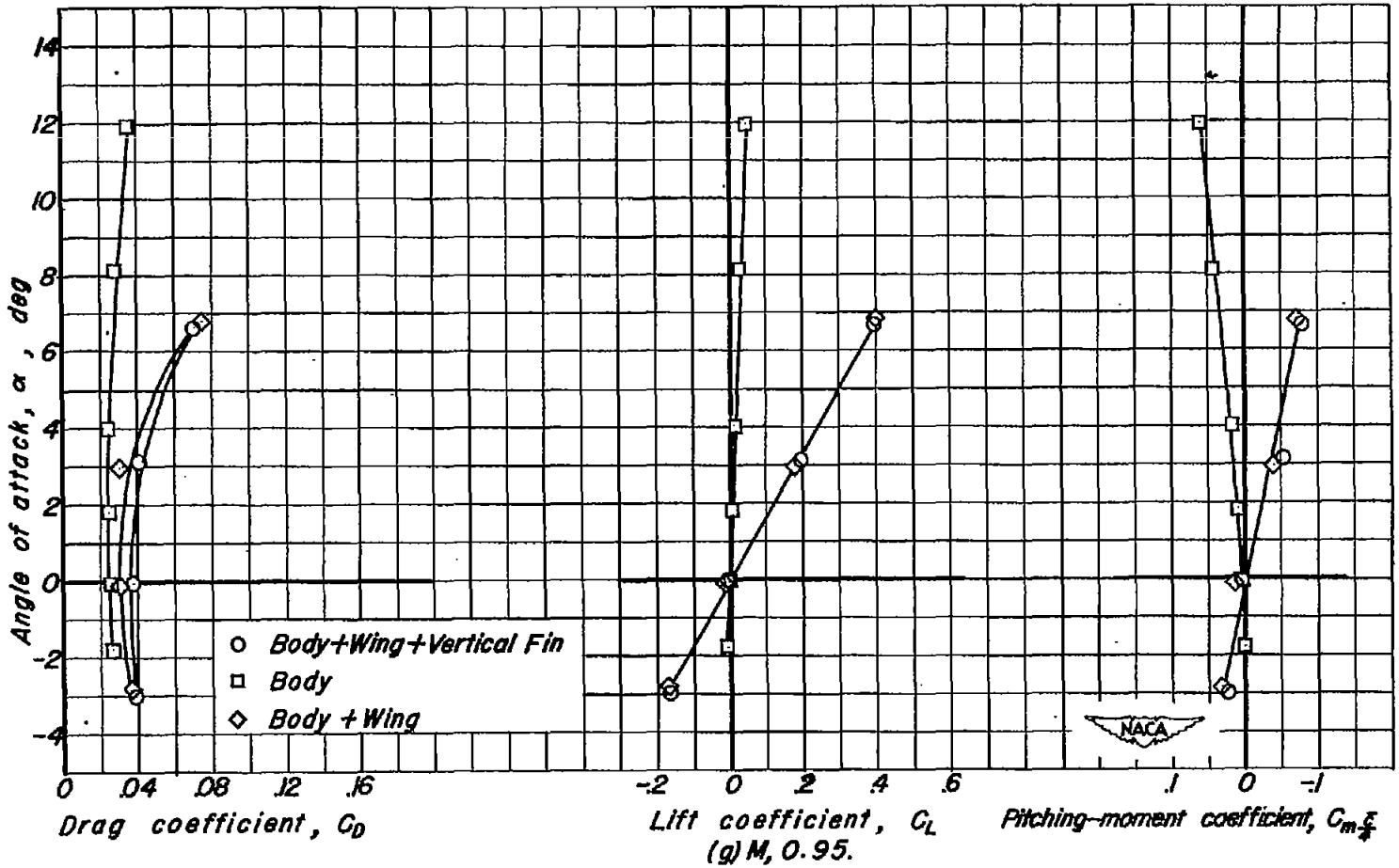

Figure 7.-Continued.

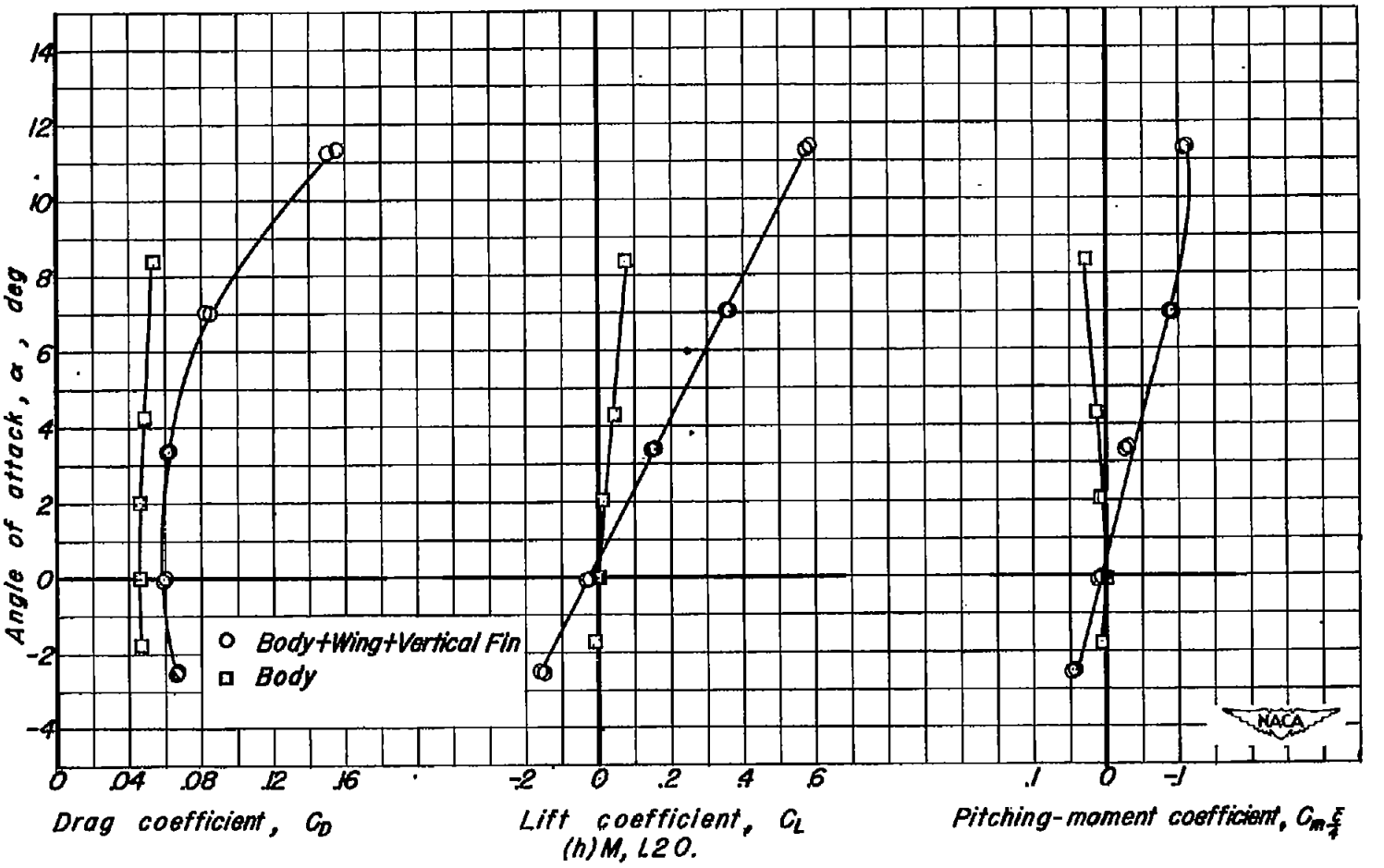

(h) M, L2O.

Figure 7.-Continued.

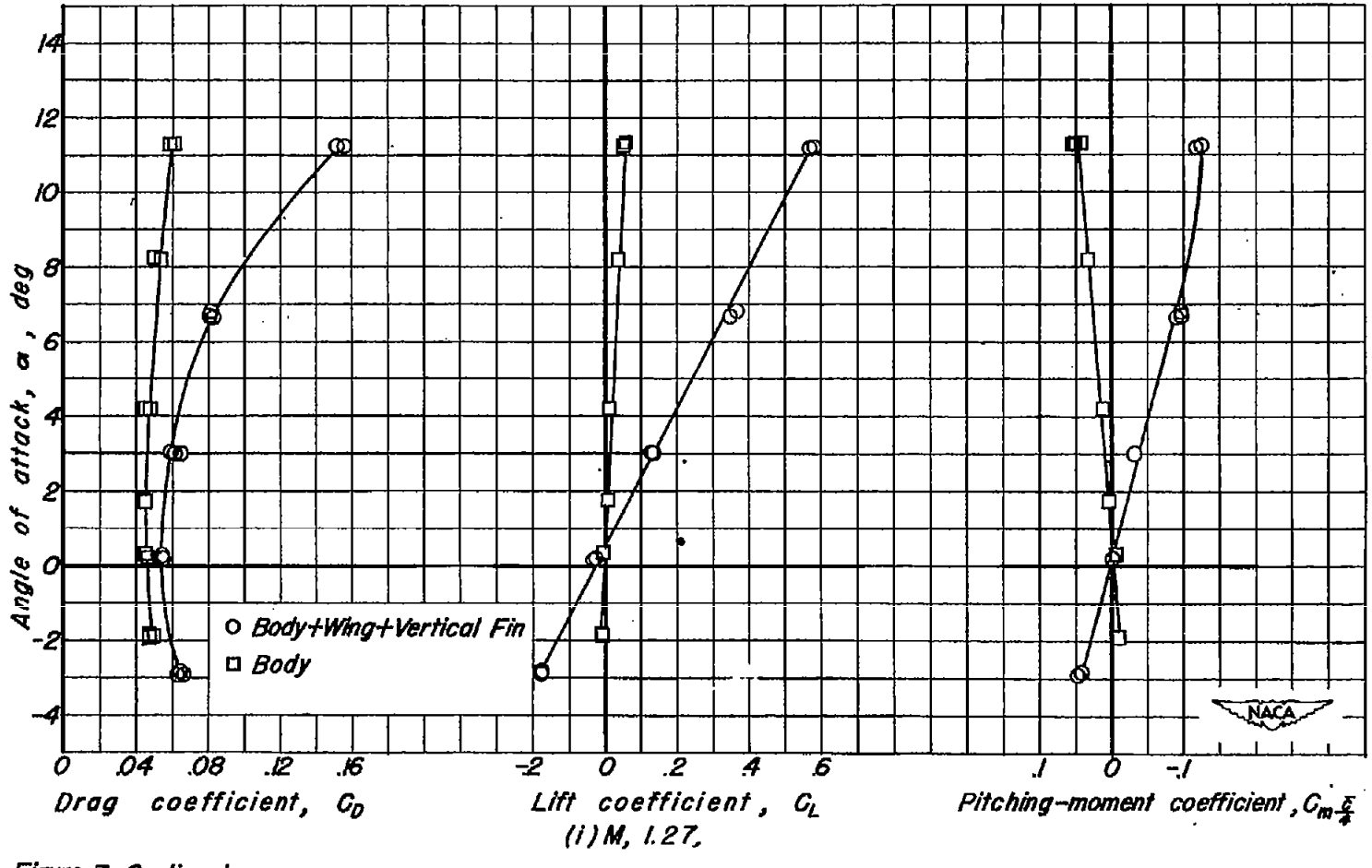

Figure 7.-Continued.

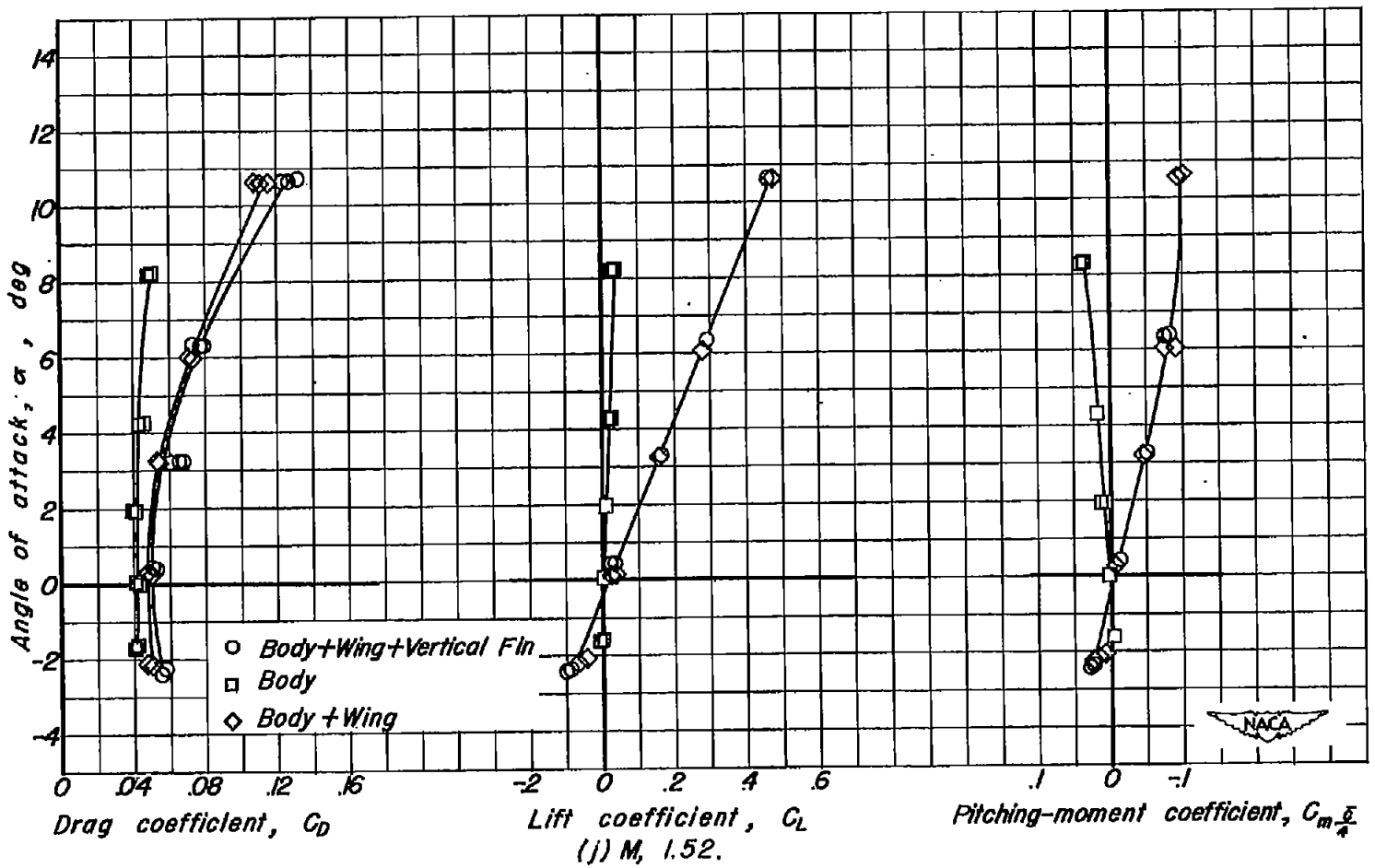

(j) M, 1.52.

Figure 7.-Concluded.

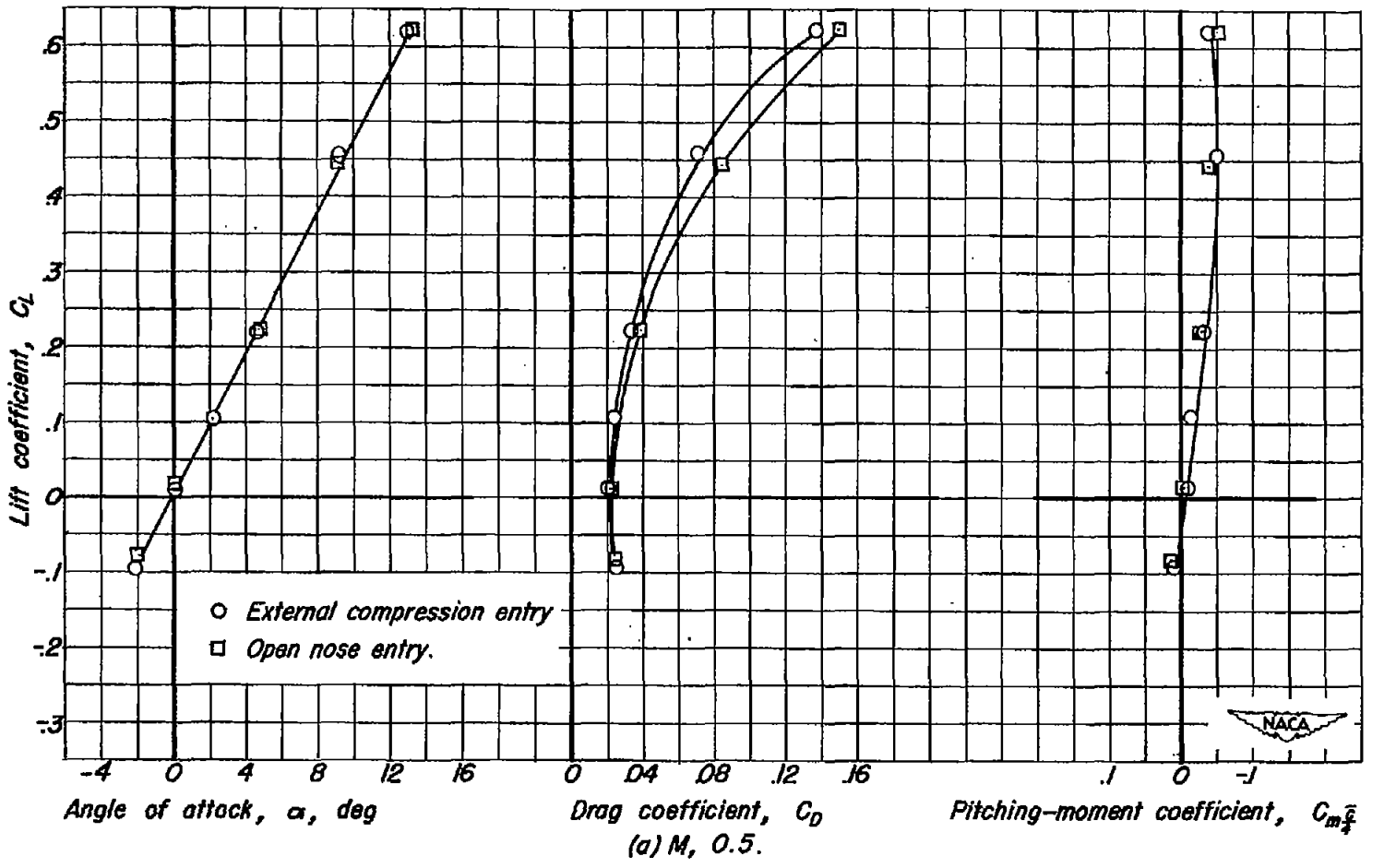

(a) M, 0.5.

Figure 8.—Variation of the aerodynamic characteristics of the complete models with external compression and open nose entries.

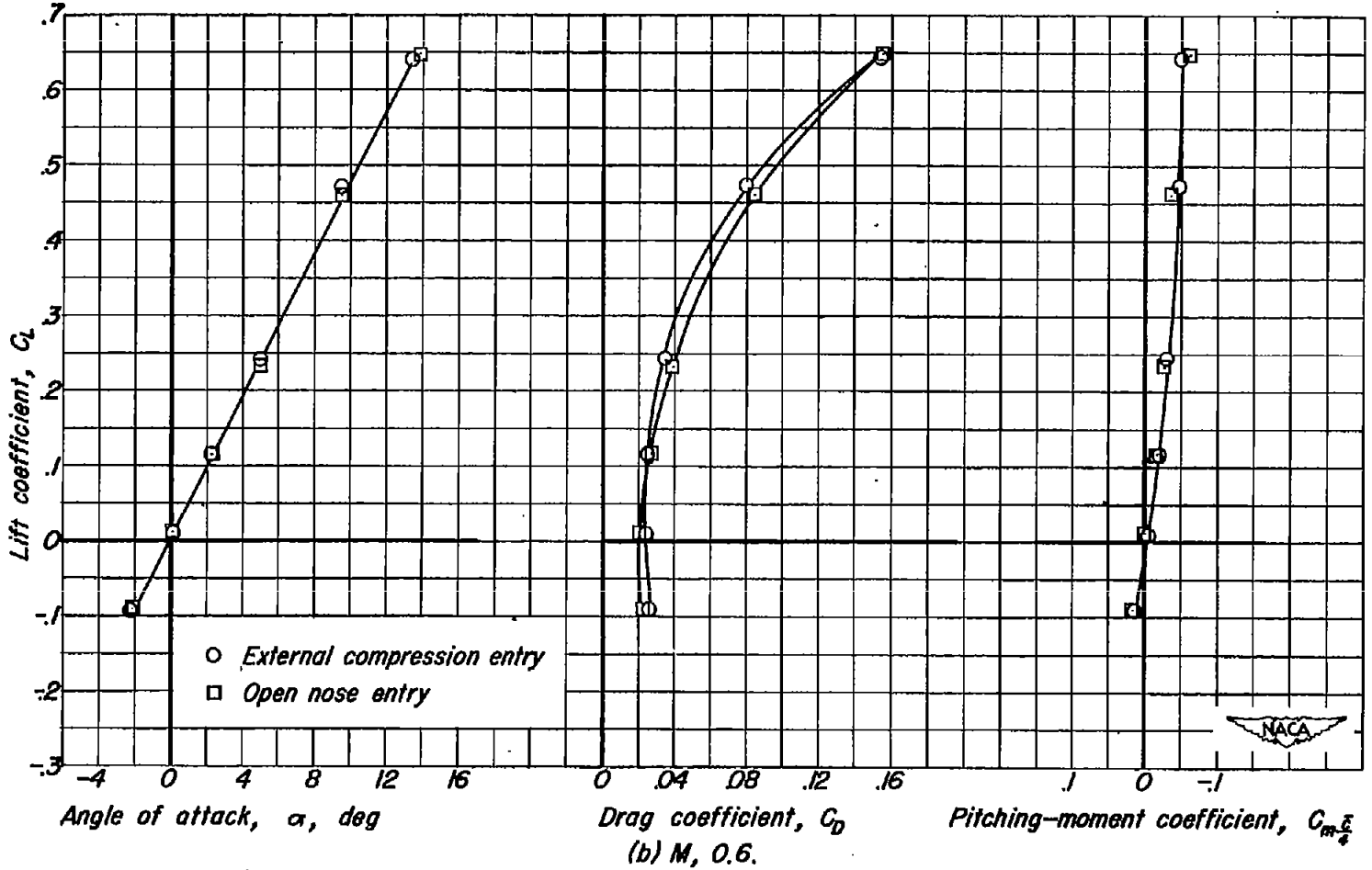

(b) M, 0.6.

Figure 8.- Continued.

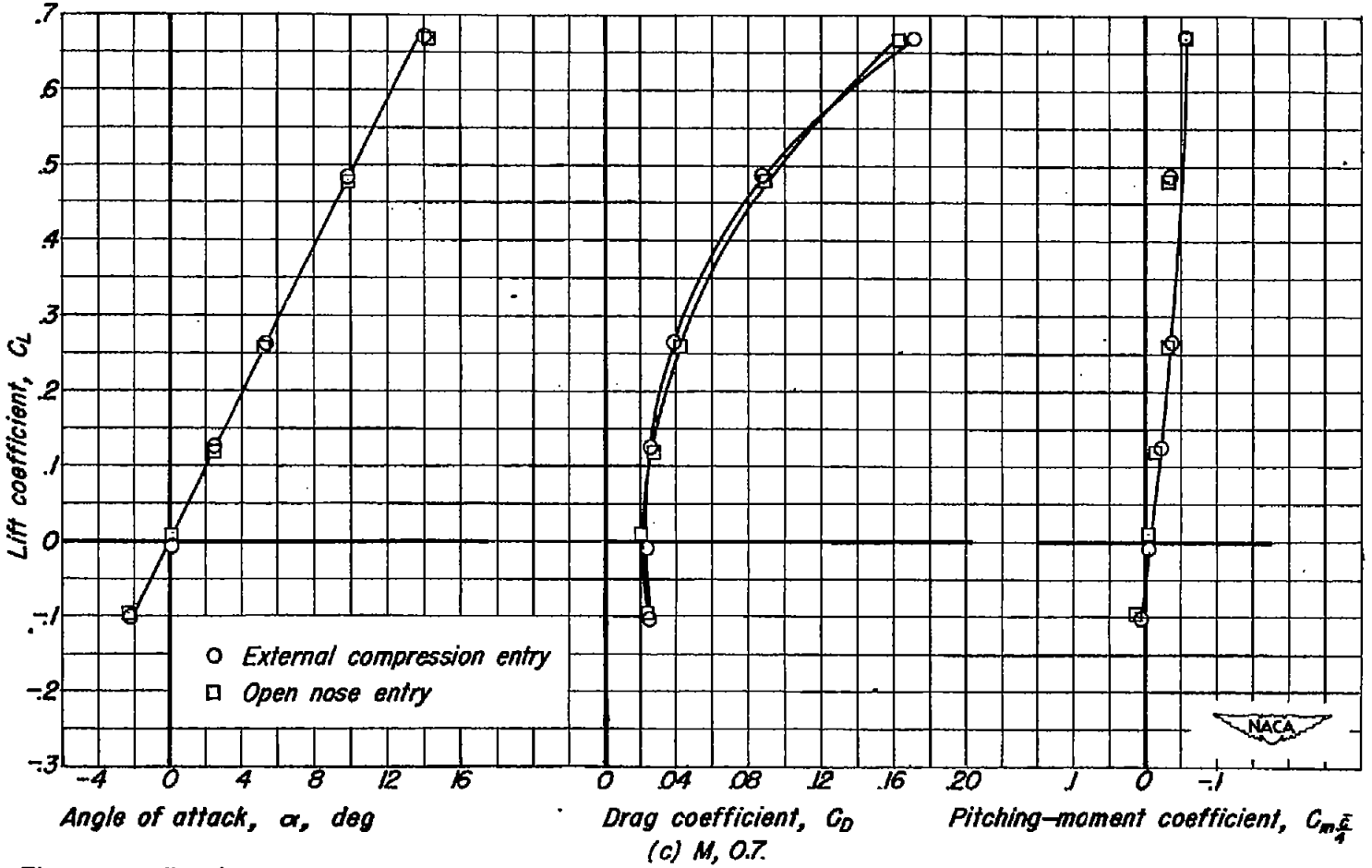

(c) M, 0.7.

Figure 8.-Continued.

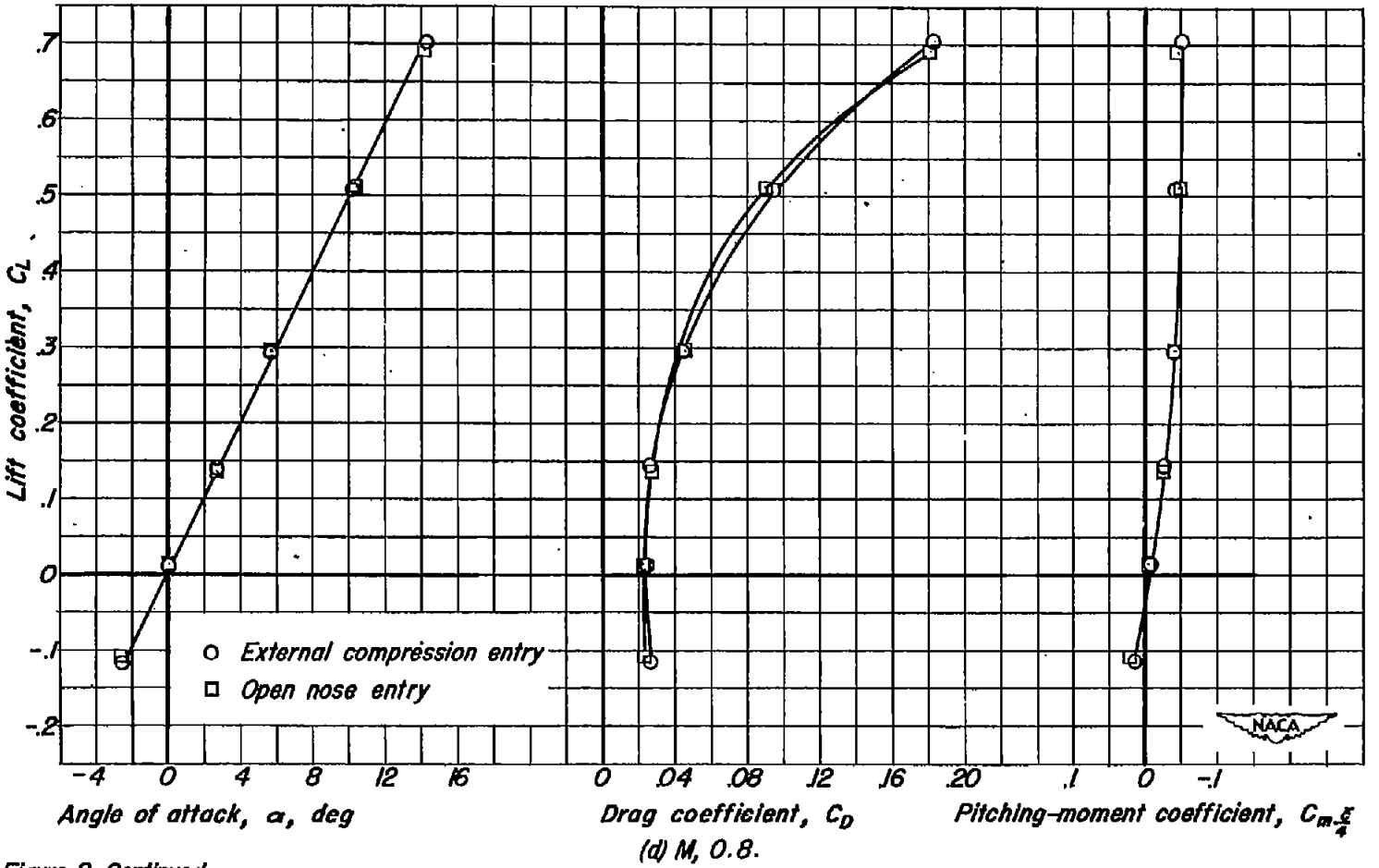

(d) M, 0.8.

Figure 8.-Continued.

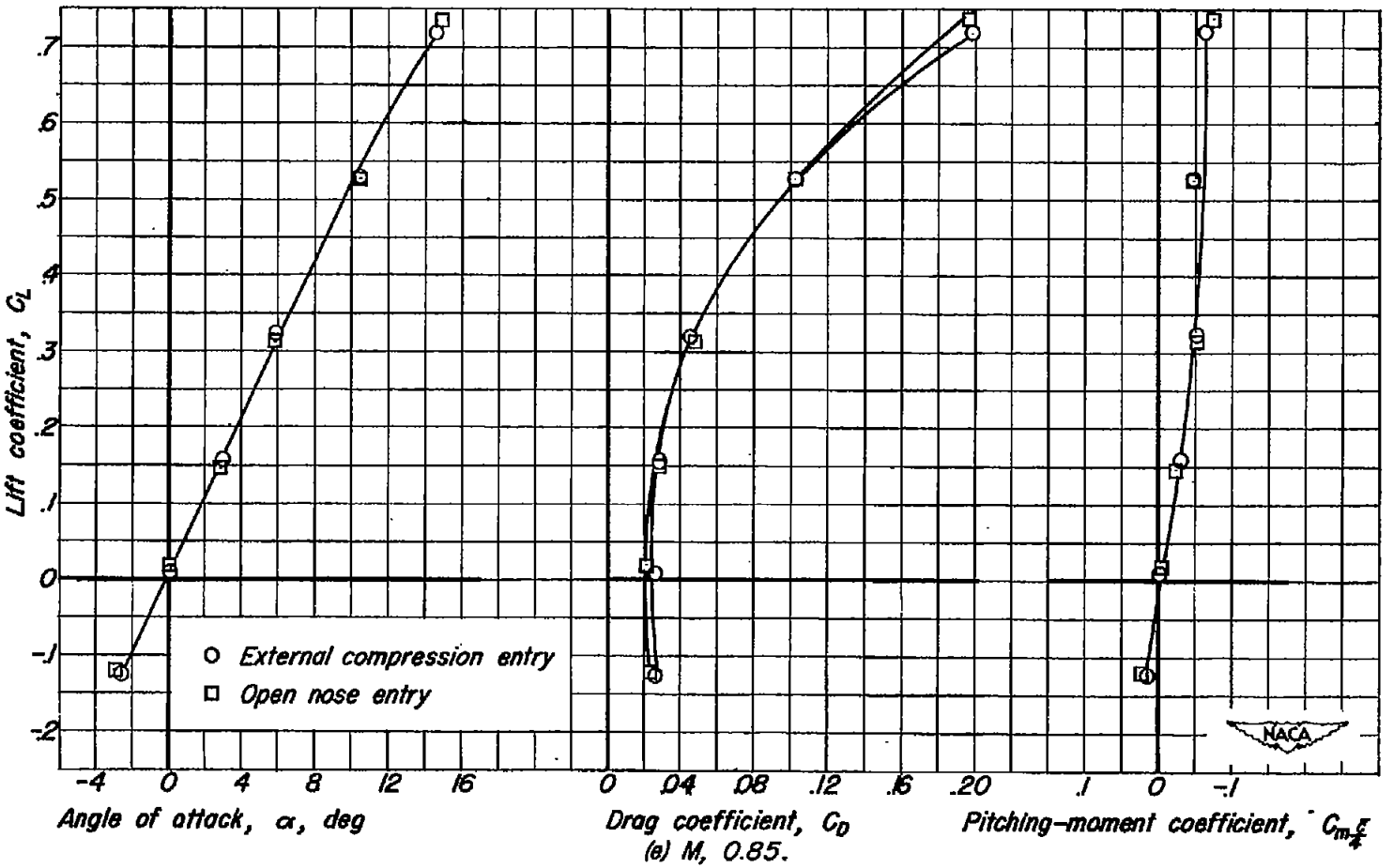

(e) M, 0.85.

Figure 8.-Continued.

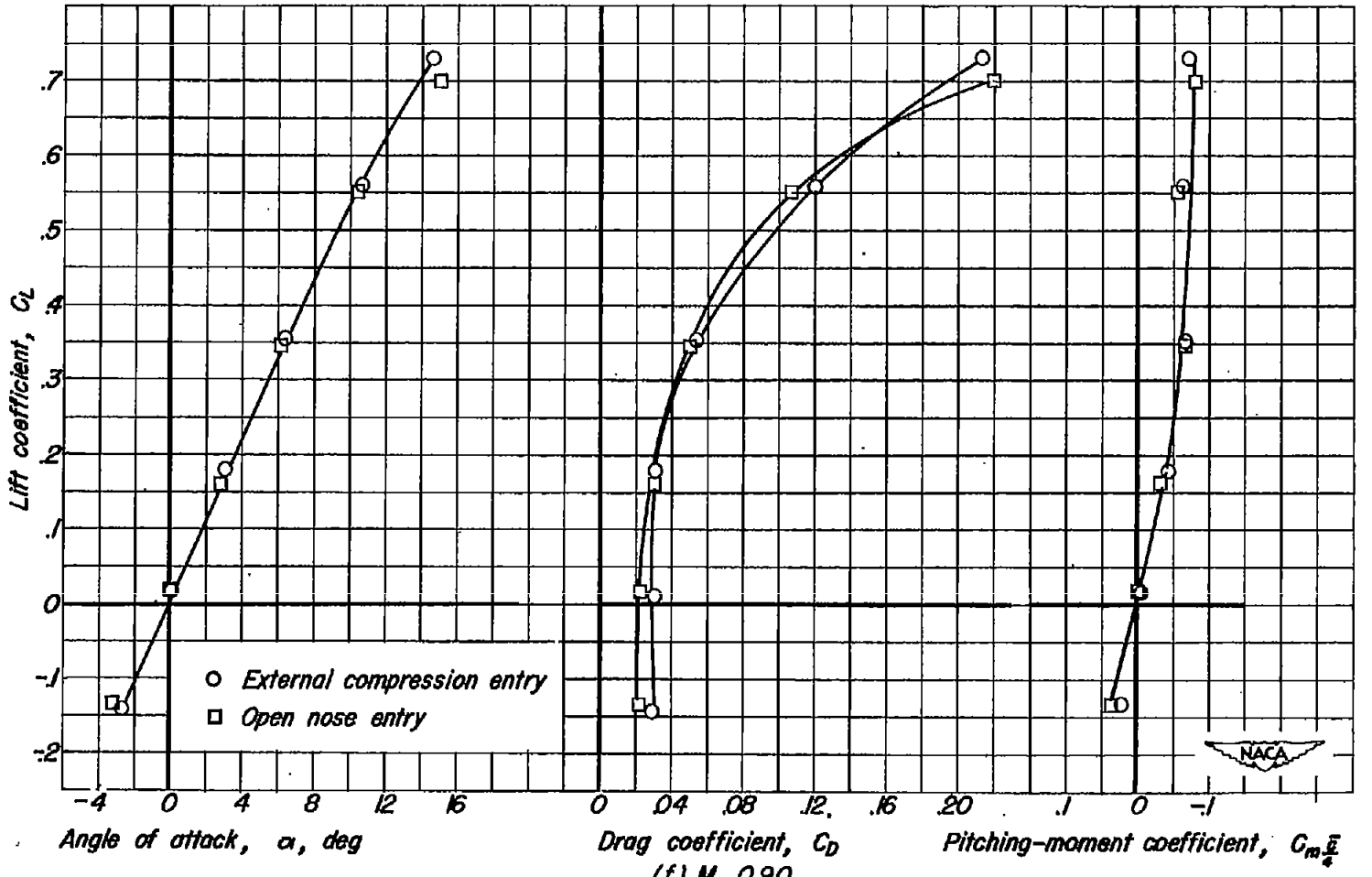

(f) M, 0.90.

Figure 8.-Continued.

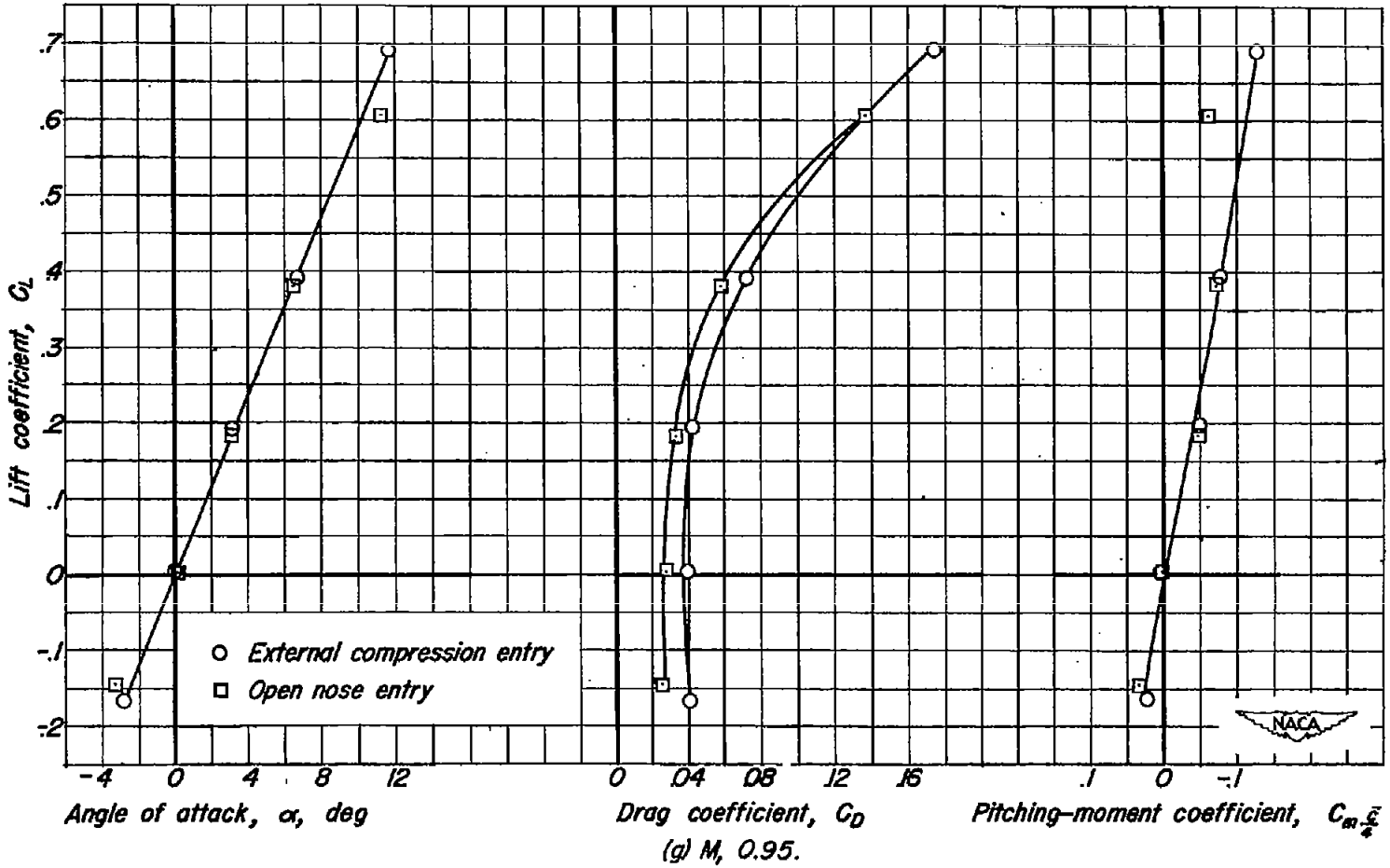

(g) M, 0.95.

Figure 8.-Continued.

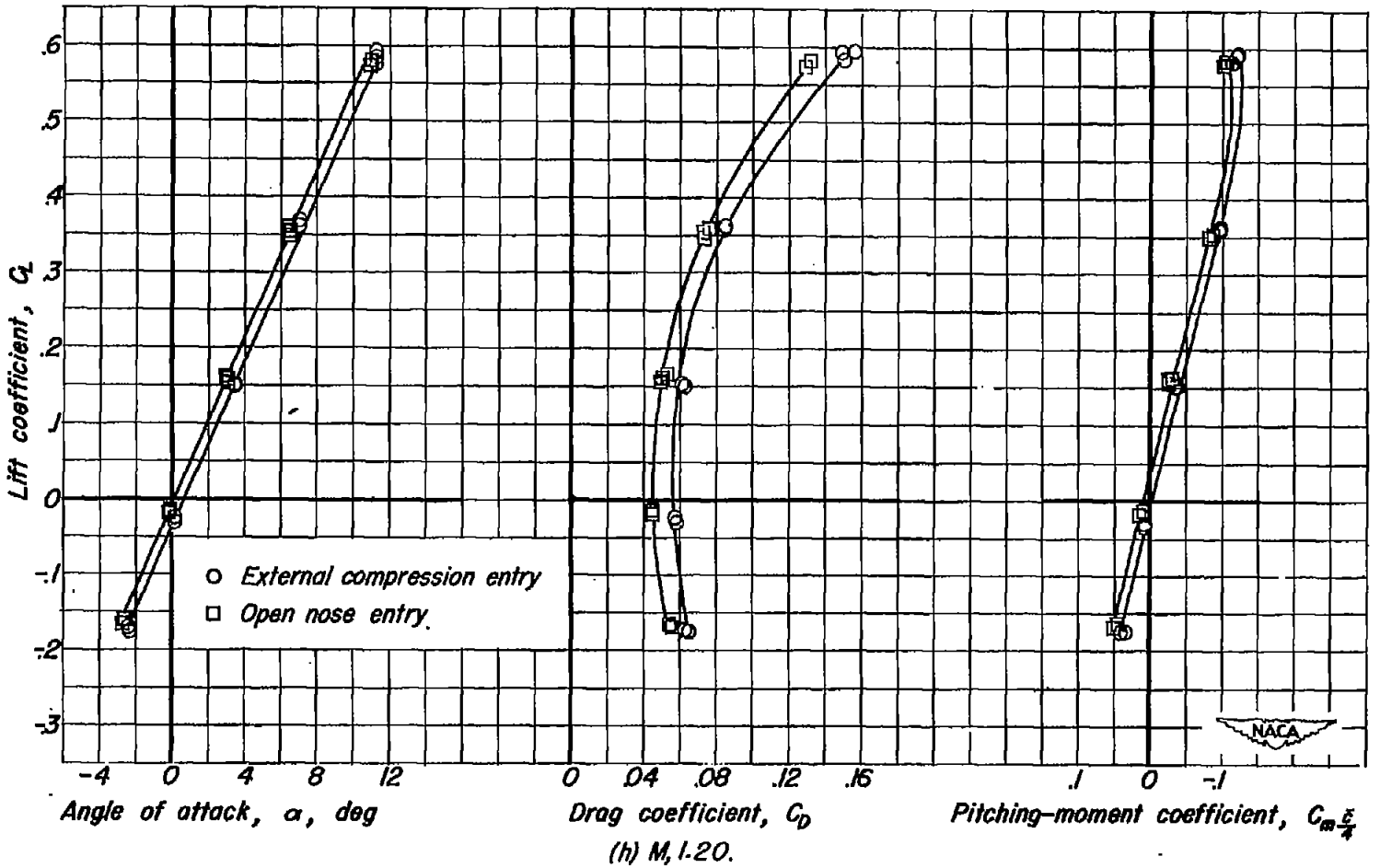

(h) M, 1.20.

Figure 8.-Continued.

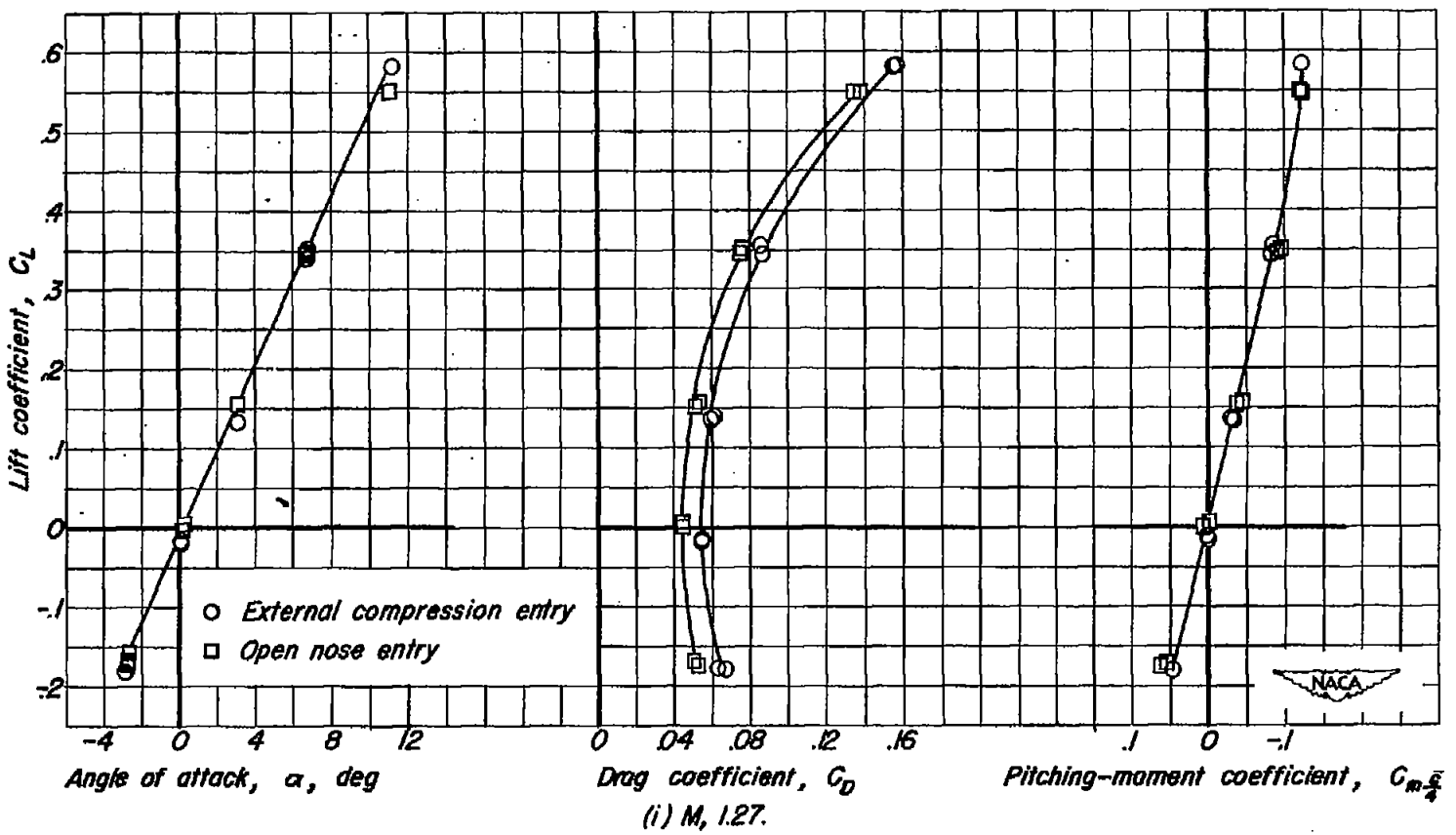

(i) M, 1.27.

Figure 8.-Continued.

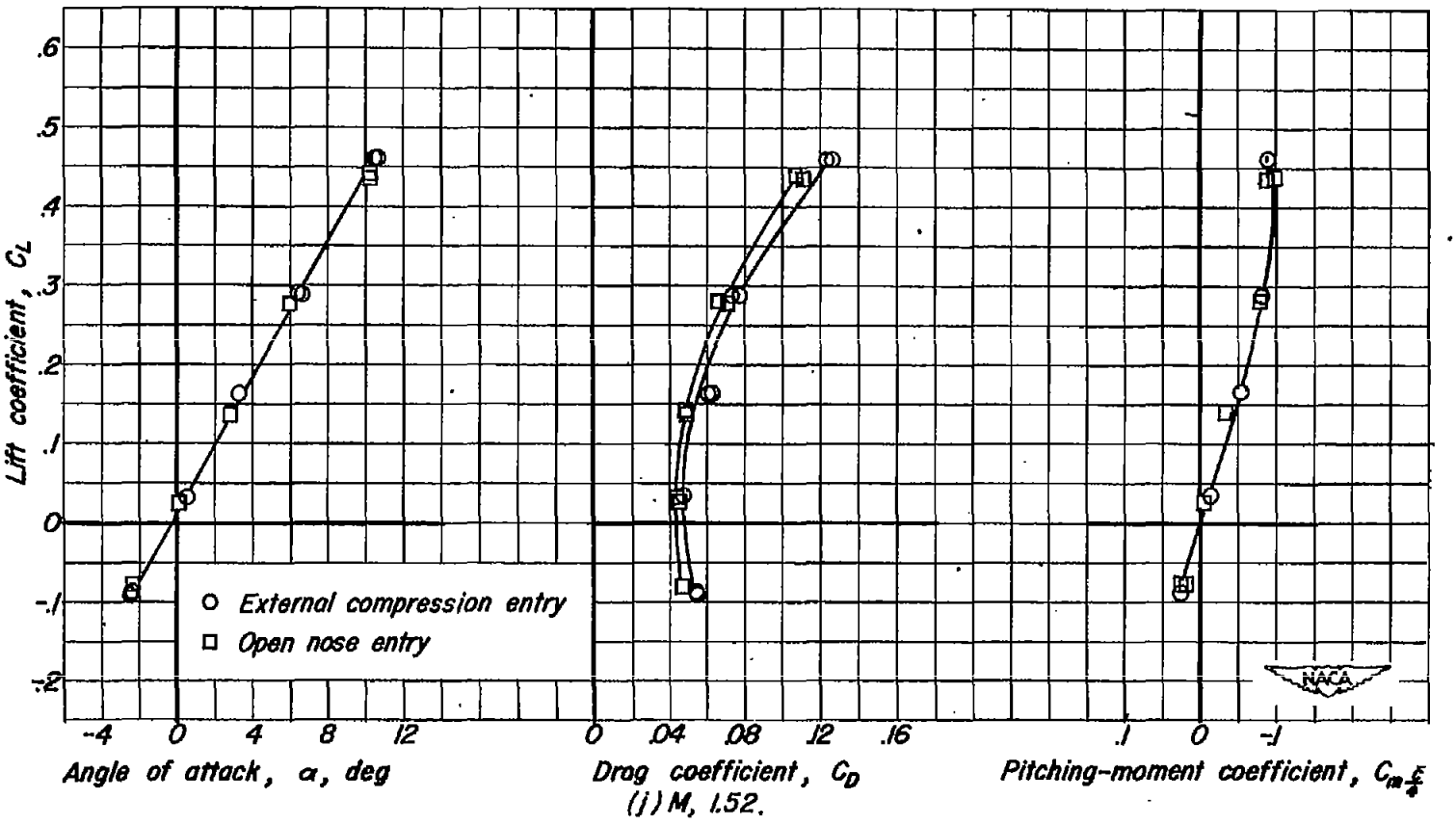

Figure 8.-Concluded.

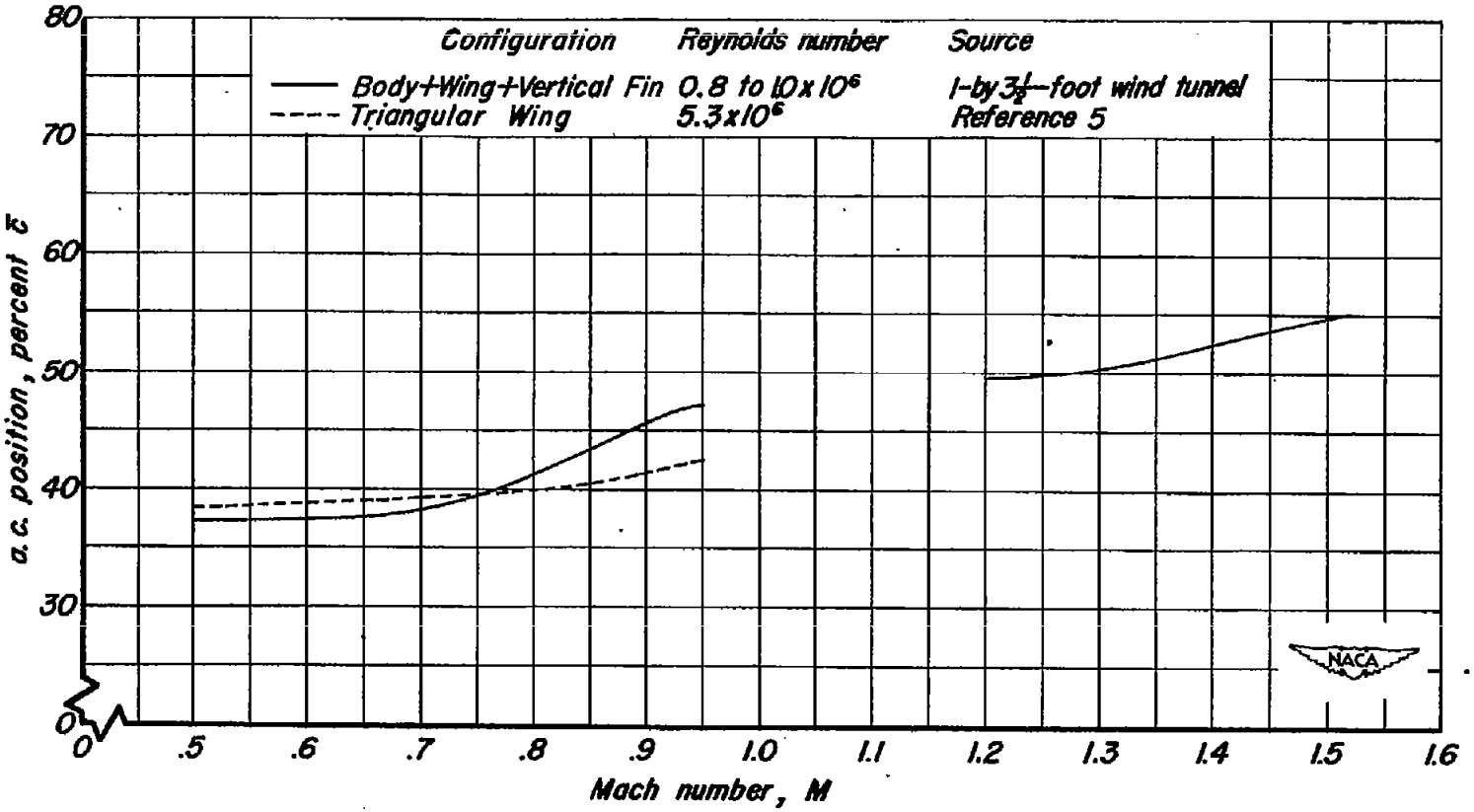

Figure 9.—Variation of the aerodynamic center of the model with Mach number.

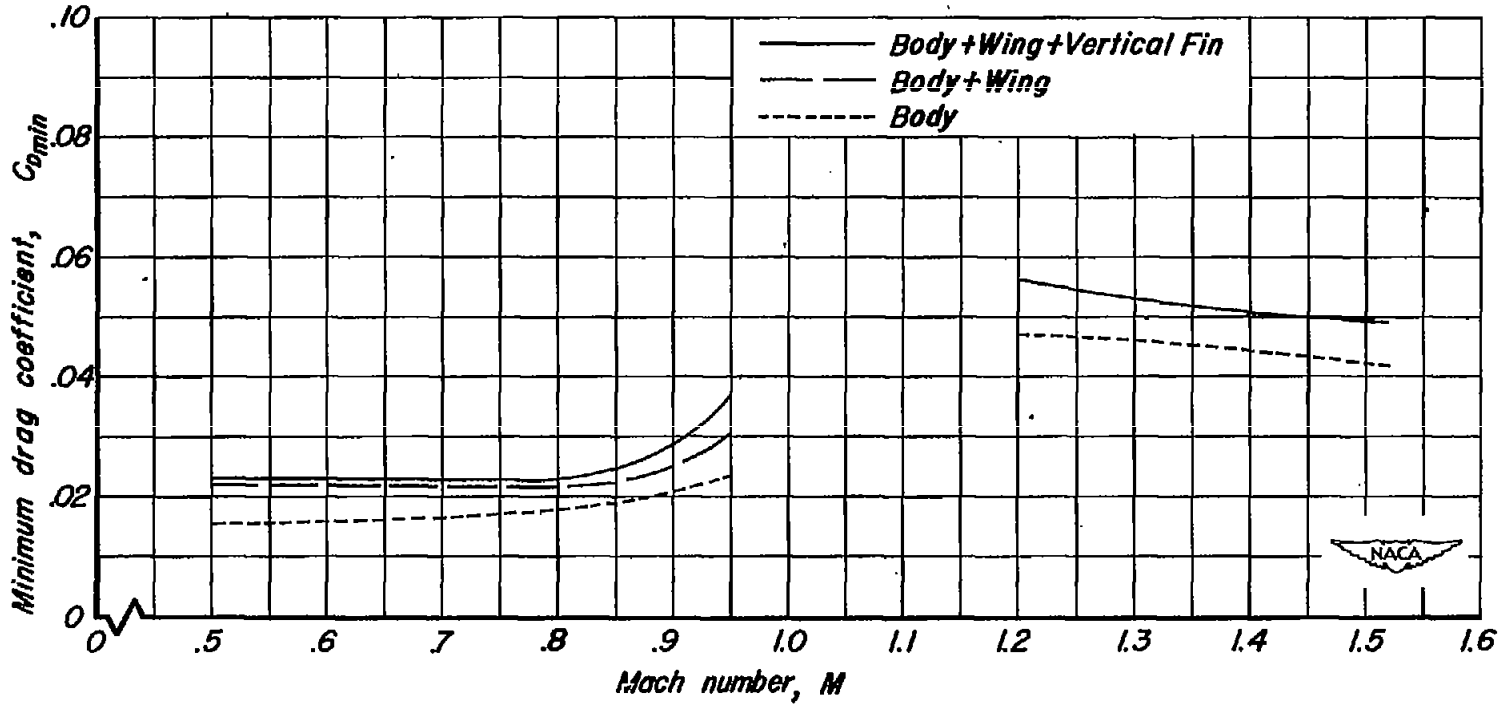

Figure 10.—Variation of the minimum drag coefficient with Mach number for components of the model with the external compression entry.

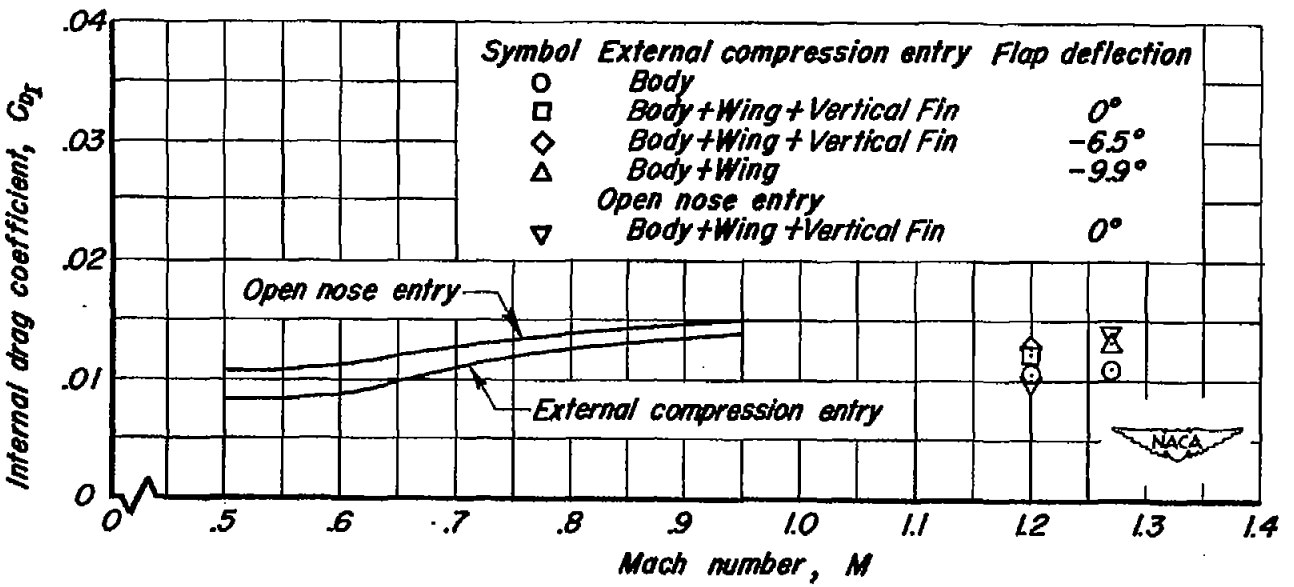

Figure 11.—Variation of the internal drag coefficient with Mach number for the complete models, except as noted.

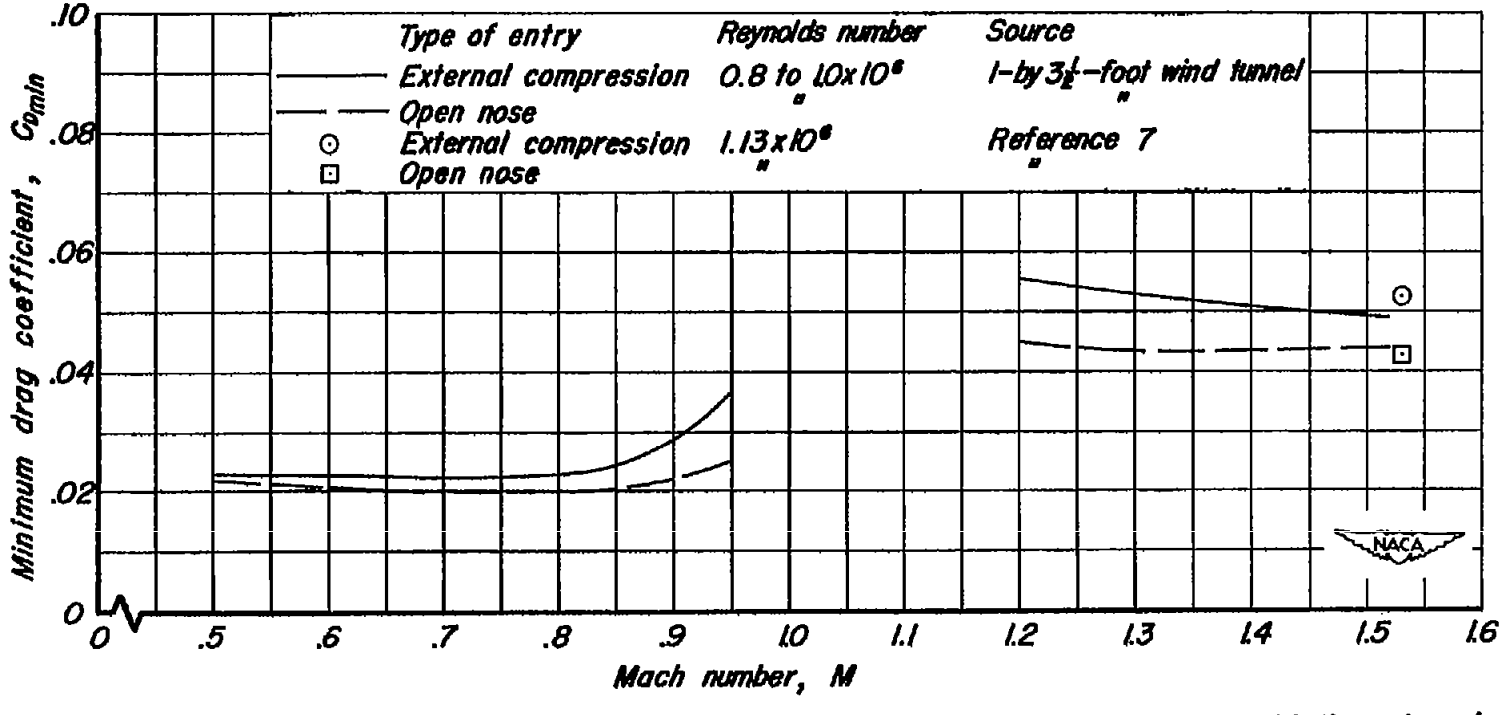

Figure 12.–Variation of the minimum drag coefficient with Mach number for the models with the external compression and the open nose entries.

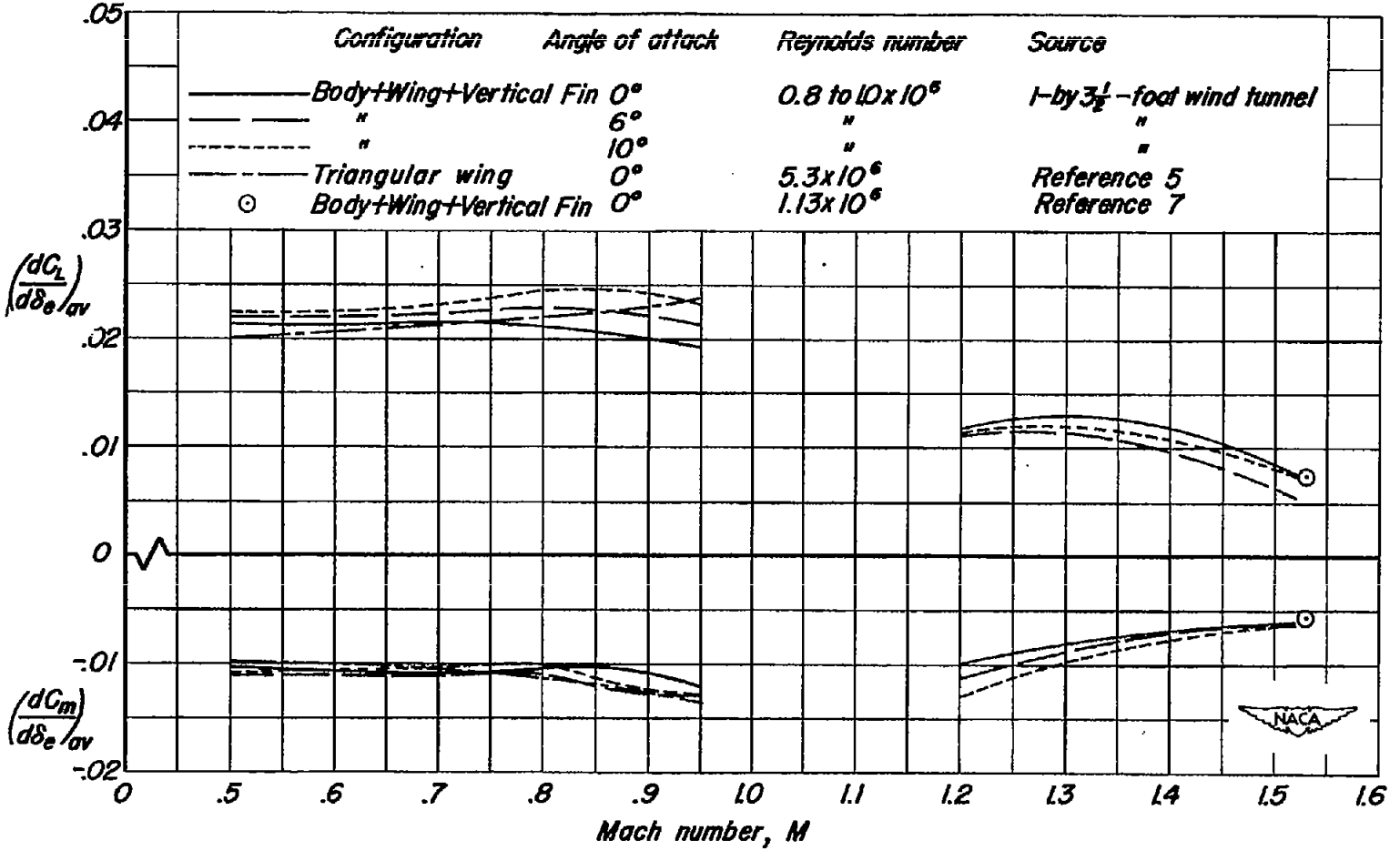

Figure 13.–Variation with Mach number of the effectiveness of a constant chord flap on the model with the external compression entry.